J Coast Conserv
DOI 10.1007/s11852-015-0397-5

Monitoring and assessing waterlogged and salt-affected areas in the Eastern Nile Delta region, Egypt, using remotely sensed multi-temporal data and GIS

Mohamed O. Arnous[1] · **David R. Green**[2]

Received: 5 March 2015 / Revised: 23 May 2015 / Accepted: 25 May 2015

Abstract Waterlogged and salt-affected soils are serious environmental hazard indicators for wasteland problems in arid and semi-arid regions of the World. Similarly human activities in agricultural and urban sustainable developments have also led to the development of waterlogging and subsequent salinization of soils leading to many geo-environmental problems. Thus, it is important to be able to monitor, assess and map waterlogged and salt-affected areas at an early stage to develop an effective soil reclamation programme that helps to reduce and prevent a future increase in areas of wasteland. Remote sensing and GIS tools and techniques have been found to outperform more traditional methods for assessing the impact of soil salinity and waterlogging, thereby providing extremely useful, informative, and professional rapid assessment techniques for monitoring and accurate mapping and the quantification of waterlogged areas and salt-affected soils. This study applies digital image processing and GIS tools to monitor, assess, and map the waterlogged and salt-affected areas, to establish the main causes that lead to widespread wastelands, and to suggest approaches to mitigation in the eastern Nile Delta region in Egypt. Multi-temporal Landsat 5, 7 and 8 data for 1984, 2000, 2006 and 2013 and ASTER GDEM were selected to monitor, assess and map the waterlogged and salt-affected areas, and to determine and map the rate of change of land-use/land-cover, the status of wasteland, and the use of geomorphological terrain analyses based on enhanced digital images processing and field verification. Image band combinations, PCA, change detection, and image classification techniques, together with many indices such as NDVI, NDSI, NDWI and NDBI were applied, together with statistical analysis, to construct various thematic and spatial distribution change maps of the wasteland hazard indicators. Spatial distribution maps of waterlogging, salt-affected areas, permanent and temporarily waterlogged areas, surface changes, and their rate of change in addition to integrated relationships between terrain analyses, water table, depth to water and landform maps over a timespan of 29 years based on the analysis and interpretation results of image processing, field investigation and ancillary geological and hydrogeological data. The results reveal that changes to land-cover caused by human activities - particularly irrigated agriculture and land reclamation as well as urban expansion - will lead to a serious deterioration in the environment through waterlogging and salinization presenting future difficulties for any sustainable development of the study area. In addition; the existence of natural factors such as areas of low-lying land, topographic depressions, and rising water tables will increase the threat of waterlogging and salinization. It is concluded that it is essential for planners and decision makers to seriously consider taking appropriate action now concerning the recommended mitigation measurements from this study to avoid serious future problems in these areas.

Keywords GIS · Salt-affected · Wasteland degradation mapping · Change detection · Classification · Indices · Terrain analysis · Land-use/land-cover

✉ Mohamed O. Arnous
arnous_72@yahoo.com; mohamed.arnous@science.suez.edu.eg; m.arnous@abdn.ac.uk

[1] Geology Department, Faculty of Science, Suez Canal University, 41522 Ismailia, Egypt

[2] AICSM, Department of Geography and Environment, School of Geosciences, College of Physical Sciences, University of Aberdeen, AB24 3UF Scotland, UK

Published online: 02 June 2015

Introduction

Monitoring and assessment of the availability and condition of geo-environmental hazard indicators based on Remote Sensing (RS), Geographic Information System (GIS) and Global Positioning Systems (GPS) is the first stage for any sustainable development plan in the world (Arnous et al. 2011; Hadeel et al. 2011; and Al-Abdulghani, et al. 2013). RS and GIS tools and techniques provide very powerful tools and techniques for surveying, identifying, classifying, mapping, monitoring, characterization, and tracking of changes in the composition, extent, and spatial distribution, surface changes and determination and assessment of different land-use/land-cover (LU/LC) classes.

The assessment process proposed in the present study seeks to determine the rates or levels of various phenomena such as waterlogging and salinization, to establish the trends in measurements or conditions, identify the causes of rates and trends; and to determine the type and impact of the consequences of rates and trends. Moreover, mitigation measurements represent the required follow-up actions of policies and directives. The four functions of mapping, measurement, modelling, and monitoring included in RS and GIS '*toolboxes*' are used to monitor and assess the environmental degradation indicators in arid and semi-arid regions. Waterlogging and salt- affected soils are the most common and serious geo-environmental hazard problems in the world and go hand in hand and due to wastelands and the loss of productivity especially in drylands. Furthermore, there are many soci-economic problems in the world, particularly in arid and semi-arid regions arising from the lack of sustainable development. Pandey et al., (2010) observed that areas with a high risk of waterlogging in the northern Bihar plains correspond to high flood hazard categories of wasteland including those caused by salinization, waterlogging and vulnerability due to poor socio-economic conditions in these areas. It is also possible to monitor and assess land salinization and waterlogging areas by enhancing multi-temporal RS data. RS and GIS tools can be very useful for accurate mapping and quantification of waterlogged area and salt-affected soils. Ultimately, this helps to provide a means to build a sound geodatabase necessary to carry out various reclamation and preventative measures for decision-makers. RS satellite data have already revealed potential for deriving information on the nature and spatial distribution of various surfaces (Dwivedi 1994; Runnstrom 2003; Symeonakis and Drake 2004; Gao and Liu 2008; Arnous and Green 2011; Arnous 2011). In the present study, the monitoring and assessment of these environmental hazards will be achieved with the aid of RS and GIS tools in order to determine the nature, spatial extent, magnitude, distribution, and temporal behavior of wastelands as the basis for successful prevention and rehabilitation measures. Many RS and GIS-based analyses of multi-temporal spaceborne data and the quantitative mapping of waterlogged and salt-affected soil hazards have been proposed since the beginning of RS and GIS applications for monitoring and assessing geo-environmental and hazards research. Many studies have recommended and envisaged RS and GIS tools for their potential to identify, delineate, map, monitor and assess waterlogging and soil salinization in arid and semi-arid regions around the world; for example: Raina, et al. 1993; Goossens, and Van Ranst 1996; Sabins 1997; Dwivedi et al. 1999; Sujatha et al. 2000; Van Lynden and Mantel 2001; Haboudane et al. 2002; Khan et al. 2005; Chikhaoui et al. 2005; Li et al. 2007; Prince et al. 2009; Gao and Liu 2010; Hadeel, et al. 2011; Singh, et al. 2012; Allbed and Kumar 2013; Kaiser et al. 2013; El Baroudy and Moghanm 2014; Singh 2015. It is also possible to study land salinization and waterlogging using RS data. Spaceborne satellite data have shown the potential for providing information about the nature and spatial distribution of various degraded land, such as salinization and waterlogging (Dwivedi 1994). Areas affected by degradation can be identified and mapped from Landsat Thematic Mapper (TM) images (Raina et al. 1993). Information on the spatial extent and distribution of salt-affected soils can be derived from Landsat multispectral scanner (MSS) data. The visual interpretation of Landsat MSS and TM images, in combination with other ancillary information and suitable ground data, can be used to determine the extent and spatial distribution of salt-affected soils, waterlogged areas and eroded lands from the visual interpretation of RS images (Sujatha et al. 2000). RS imagery is beneficial for revealing the land that has been affected by degradation to various degrees (Gao and Liu 2008). The degraded land can be mapped with more than 70 % accuracy from ASTER data using both per-pixel and object oriented image classification methods (Gao 2008). A spectral index derived from Advanced Spaceborne Thermal Emission and Reflection Radiometer (ASTER) data has been suggested to characterize the state of land degradation (Chikhaoui et al. 2005). Moreover, the waterlogged areas can also be mapped from a 1:50,000 Landsat Thematic Mapper (TM) false colour composite print. And also, the waterlogged areas and salt-affected soils were delineated from Indian RS Satellite (IRS)-1B Linear Imaging Self-scanning Sensor (LISS-I) and Landsat TM data via visual interpretation (Dwivedi et al. 1999). RS multi-temporal data are effective in identifying and mapping land degradation risks in areas under human-induced stresses, Western Brazilian Amazon (Lu et al. 2007). In particular, RS satellite data can effectively reveal the spatial extent, magnitude and temporal behavior of lands that are affected by waterlogging and subsequent salinization/alkalinization (Sujatha et al. 2000), even though it may be difficult to retrieve RS primary parameters such as reflectance (Hill et al. 1995; and Khan et al. 2005). The spectral classification of salt-affected and waterlogged areas characterization were carried out with the aid of

digital data analysis and GIS. Permanently and seasonally waterlogged areas were successfully mapped with RS data (Chaube 1998; Dwivedi and Sreenivas 1998a, 1998b; Mandal and Sharma 2001, 2011). RS and digital terrain models, detailed catchment mapping, and groundwater levels coupled with landform maps were integrated to monitor and estimate the extent and potential area of salt-affected land. The results of this monitoring have a number of advantages: firstly, they show the location of salinity within catchments and hazard areas at a regional scale, and allow for more efficient identification than using any other method (McFarlane et al. 2004). By using RS and GIS techniques, Li et al. (2007) identified LU/LC changes between salinized wasteland and other land-cover types in the Western part of Northeast China over the last 50 years. The spatial distribution of regional patterns of land degradation can reliably be mapped by using the indices describing the spectrum shape and spectral unmixing (Haboudane et al. 2002). When combined with topographic variables, spectral information is very useful for land degradation assessment. Due to its extensive distribution, land degradation is ideally monitored by means of RS providing information on vegetation cover, rain use efficiency, surface runoff and soil erosion. The combined use of such information highlights the areas highly susceptible to degradation (Symeonakis and Drake 2004). By monitoring changes in grassland biomass production and reclamation activities, Runnstrom (2003) detected the nature and scale of land degradation in the Mu Us Sandy Land of north central China. Furthermore, Chen and Rao (2008) carried out monitoring change by mapping the land degradation in a transition zone between grassland and cropland in northeast China using multi-temporal landsat TM/ETM data.

RS multispectral data, by virtue of providing synoptic views of fairly large areas at regular intervals, have been found to be very effective in providing information on salt-affected soils and waterlogged areas in a timely and cost-effective manner (Bouwer et al. 1990; Dwivedi et al. 2001). The use of long-term multi-temporal satellite data to monitor and assess the changes in the spatial distribution of waterlogged and salt-affected soils is usually accomplished by using change detection techniques. It includes an investigation of the differences between two surface models that are acquired at specific timespans. A number of change detection techniques have been developed for this purpose, such as transparency compositing, image differencing, post classification comparison, band ratioing, and principal components analysis (Mouat et al. 1993; Khalifa and Arnous 2012). Although image differencing and image ratioing are relatively easy to apply, these change analysis methods -based on raw pixel values - require the selection of an appropriate set of thresholds for measuring change. These thresholds are empirically derived to differentiate changes from background variations, which can be rather challenging in some cases. By comparison, post-classification change detection allows for the identification and mapping of amount, and the location and nature of differences in land-cover (Rubec and Thie 1980). LU/LC change maps, derived from post-classification comparison, generated information on the spatial distribution and type of LU/LC changes (Phinn and Stanford 2001; Arnous and Green 2011; Juman and Ramsewak 2013). Furthermore, the post-classification comparison technique is the most accurate among image differencing, vegetative index differencing, Selective Principal Components Analysis (SPCA), direct multi-date unsupervised classification, post-classification change differencing and a combination of image enhancement and post-classification comparison (Mas 1999). However, it is unknown how accurate changes are when detected using post-classification.

Increasing population, rapid industrial development and agricultural expansion in new areas usually requires additional water resources. Whilst water demands will continue to increase, the fixed amount of fresh water resources available will always impose a challenge. Due to the increasing population, successive governments in Egypt have encouraged agricultural expansion and the establishment of new communities in the desert fringes of the Nile Valley. When initiating a new community or a major agricultural project in a desert area, the major challenge is to maintain sustainable water resources and waste management programs. In addition, large investments in land reclamation have targeted the sandy flood plain east of the Nile Delta because of the good potential for water resources and transportation accessibility. In Egypt, groundwater is the second most important water resource after the Nile River, and recently its development and management have become extremely important. In the Eastern Nile Delta region, the land reclamation projects in the desert fringes and coastal zones started in the early fifties but have increased rapidly since 1980.

Today, waterlogging and salinization go hand-in-hand, and have become huge threats in some locations of the East Nile Delta where agricultural land has become totally barren, and in some others, the soil has become saline. The prevailing hydrogeological conditions, in association with poor land-use planning, and the role of geological and geo-environmental factors determines the strategy of land reclamation and sustainable development and the most likely causes of the above problem. The study area investigated represents a promising area for different types of development since it is one of the nearest areas to the Nile Valley and Nile Delta, rich in resources and bounded by four major Governorates including, Great Cairo, Suez, Ismailia, and Sharkiya. During the last three decades, there was considerable interest in developing the Sinai Peninsula (Fig. 1). This could partially help in solving some of the economic and social problems of Egypt and, in addition open up new opportunities for more development and investment mainly in the Sinai Peninsula.

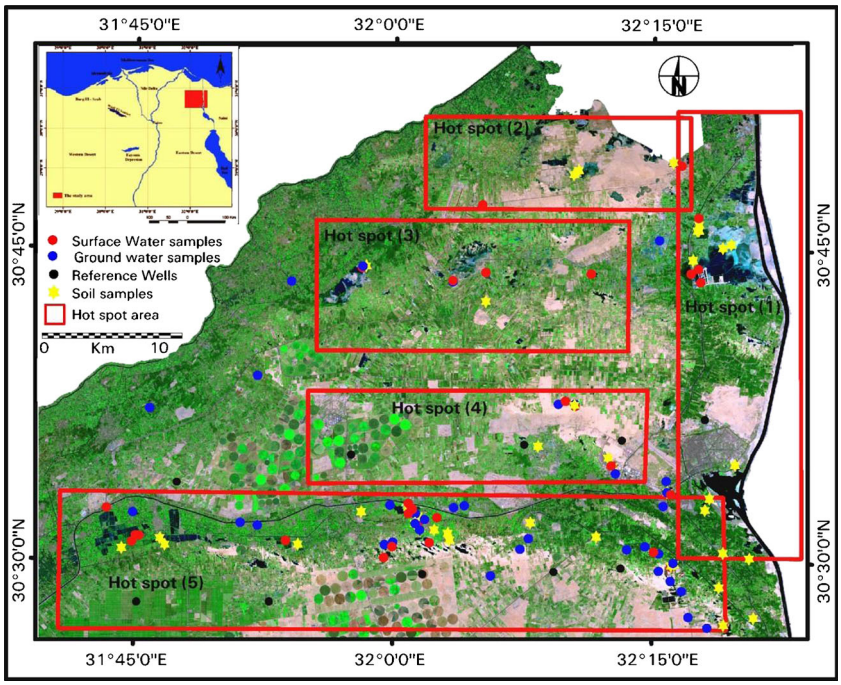

Fig. 1 Location, sampling and hot spot sites map of the study area

The major problems of the present study area are characterised by land degradation in cultivated and reclaimed land areas, something that is predicted to become a serious and extensive environmental problem in the next few years. Waterlogging and soil salinization are the prevailing forms of land degradation in the low lying lands of the study area. This problem is very persistent in the study area where infrastructure is currently drowning through the waterlogging of cultivated lands, houses, roads, electricity towers and industrial zones as well as from environmental pollution. All of these problems will be observed and reported through field investigations and the use of enhanced satellite imagery in this study.

The present study aims to apply advanced RS and GIS technologies to study, monitor, assess and map the susceptible locations and the dynamic behavior of the waterlogged and salt-affected areas. In addition, it seeks to determine the main causes of waterlogging and soil salinization in the eastern Nile Delta. The temporal status of waterlogging and salt-affected can be obtained using the available multi-temporal satellite data to produce waterlogged and salt-effect potentiality maps within the time span of 1984 to 2013.

Characteristics of the study area

The study area covers an area of around 2425 km^2 and is located in the north-eastern part of Egypt, approximately between the latitudes 30° 27\ 18\cr – 30° 55\ 10\cr N and longitudes 31° 40\ 42\cr– 32° 20\ 54\cr E (Fig. 1). It is bounded in the North by the Mediterranean Sea and Lake Manzala, and in the south by the desert rolling plains and foot hills of tertiary and cretaceous structural ridges varying in altitude between 200 and 800 m a.s.l. On the west it is bounded by Damietta Nile Branch while, the Suez Canal represents its current eastern boundary.

The east Nile Delta is occupied by sedimentary rocks belonging to the geologic time periods of the Quaternary and late Tertiary. The eastern Nile Delta Flank constitutes about 1 % of the Egyptian land that is totally covered by Quaternary deposits of silt, clay and sands with thicknesses varying between 200 m in the south and 700 m in the north. The floodplain fans out with a gentle slope of the order of 0.3 m/km and then plains with a very low gradient to the north through a distance of about 160 km. Lake Manzala and its surroundings, are characterized by wetlands connected via a narrow link with the Mediterranean Sea. The topography of the eastern Nile Delta area is characterized by low relief, and the surface slopes gently towards the north, whilst it assumes a rolling shape towards the south where the land rises up to a moderately elevated plateau with elevations ranging between 5 and 100 m. The geomorphology of the eastern Nile Delta consists of two deltaic plains: the modern deltaic plain comprises the main portion of the fertile and cultivated land; and the old deltaic plain that stretches to the east and south of the modern floodplain. Some depressions are encountered to the south such as, Wadi El-Tumilat, and the Asthmus depression to the east. Sea level rise also has a bearing on the coastal recession and hydro-environmental degradation of the northern parts of the study area. ASTER GDEM of the study area reveals that the elevations at the eastern Nile Delta area decrease in a northward direction, and ranges between less than 2 m at the north and about 98 m in the south. The structural framework of the study site is crossed by two main fault groups

comprising ENE-WSW and NNW-SSE directions. The ENE-WSW faults have produced a number of parallel morphotectonic basins controlling the depositional regime, thickness and configuration of the overlying Quaternary sediments and determine the main water bearing formation (El-Shazly, et al. 1975). The climate in the eastern Nile delta region is characterized by an arid climate; hot, dry and rainless in the summer and mild with some showers in winter. Mean monthly temperatures range from about 12 ° C in winter to 29 ° C in summer. The average annual rainfall ranges between 20 and 100 mm. The daily evaporation varies from approximately 1.5 mm in December to 7.5 mm in July and the evaporation from open water is about 1600 mm/year (Egyptian Meteorological Authority 2006; and Nosair 2011).

Materials and methods

The importance of RS and GIS technologies for mapping, monitoring and the assessment of environmental hazards in arid and semiarid regions is extensively recognized and well-developed in a wide variety of fields. Consequently RS data is widely applied as a solution and treatment of various environmental problems. The technology can be used as an effective aid in environmental hazard investigations, as well as for environmental planning, terrain analysis such as LU/LC, geomorphology, waterlogging, salt-affected, land degradation, and terrain analyses that can also be derived from the data. Furthermore, existing information can be updated to enable the quantification of human interference on the earth's surface. Spatial and temporal thematic maps and ground-based information needs to be integrated to make decisions about the sustainable development of any area in the world. Software such as ERDAS Imagine, ArcGIS and PC ArcInfo have been used. Three types of RS data were used in the present study to monitor and assess the waterlogged and salt-affected areas and the environmental degradation of the LU/LC surface. These are multi-temporal RS Landsat satellite images (WRS2: path 176 / Row 39) obtained from NASA for the period 1984, 2000, 2006 and 2013, with cloud-free scenes acquired in the late summer season (Fig. 2). The TM (September 1984) and ETM+7 (August 2000 and 2006) and Landsat 8 OLI (August 2013) datasets were assembled and analyzed to monitor and assess the waterlogged and salt-affected areas to provide environmental degradation indicators in the study area, and in addition for the preparation of spatial distribution maps comprising different thematic maps for analytical use in the present study. The spatial resolution of the TM, ETM and OLI images was 30 m by 30 m. In addition, ASTER GDEM data were available for a pixel pitch of 30 m and a planimetric accuracy of 30 m and altimetry of 20 m from the Terra ASTER satellite. These were integrated in a GIS to carry out terrain analyses and for the mapping of the different landforms to investigate the probable sites that will be lead to the development of waterlogging hazards in the study area. This data can be combined with multispectral images to realize a better view of the landscape. The pre-processing of these datasets included image registration, radiometric calibration, and radiometric normalization. The images were geo-rectified and corrected to the WGS84 datum and the UTM N36 projection. Atmospheric correction was performed using the Dark-Object Subtraction technique (Chavez 1996). The Landsat imagery was radiometrically calibrated for sensor differences, converted into spectral radiance and normalized for illumination properties by using differences in the sun-elevation angle and sun–earth distance and recalculating the pixel values into *'at-satellite'* reflectance. All the RS data processing was performed using ERDAS Imagine 2013 for the image processing and ESRI ArcGIS 10.1 software for analyzing, integrating, and visualising the results.

Geo-referenced, tabular, and ancillary data - including topographic, geological, soil maps, socio-economic data, meteorological data - and all the thematic layers were generated in the GIS to provide confirmation for the enhancement of the RS data and as the basis for building geographical database. Fieldwork was undertaken to establish the relation between the enhanced images features and different categories of the salt–affected and waterlogged soils. In addition, the observation sites within the hotspot areas, terrain conditions, hydrogeological conditions, physiography, soil properties LU/LC, surface drainage, and groundwater table were also observed and recorded (Fig. 1).

Two goals and stages were followed. In the first stage, remote-sensing and GIS techniques were used to monitor and assess surface land changes and to determine the type of LU classes. In the second stage, the area was evaluated for environmental change in the waterlogging and salt-affected areas by using a well-known land-degradation indicator method and GIS tools, and subsequently the analysis of the impacts of LU/LC class expansion on environmental degradation hazards and any sustainability development planning. The digital image processing techniques applied involved data manipulation such as image contrast stretching, spatial filtering, change-detection, post-classification comparison, histogram matching and terrain analysis techniques. In addition, three methods were used to retrieve class boundaries, namely, supervised and unsupervised classification (a maximum-likelihood classification), Principal Components Analysis (PCA), and indices. The four indices covered were used as the bias to establish vegetation changes. These were the Normalized Difference Vegetation Index (NDVI), Normalized Difference Built-up Index (NDBI), Normalized Difference Water Index (NDWI), and Normalized Difference Salinity Index (NDSI) which were calculated and applied to the multi-temporal satellite images of the study area. GIS techniques were then used to represent and visualise the

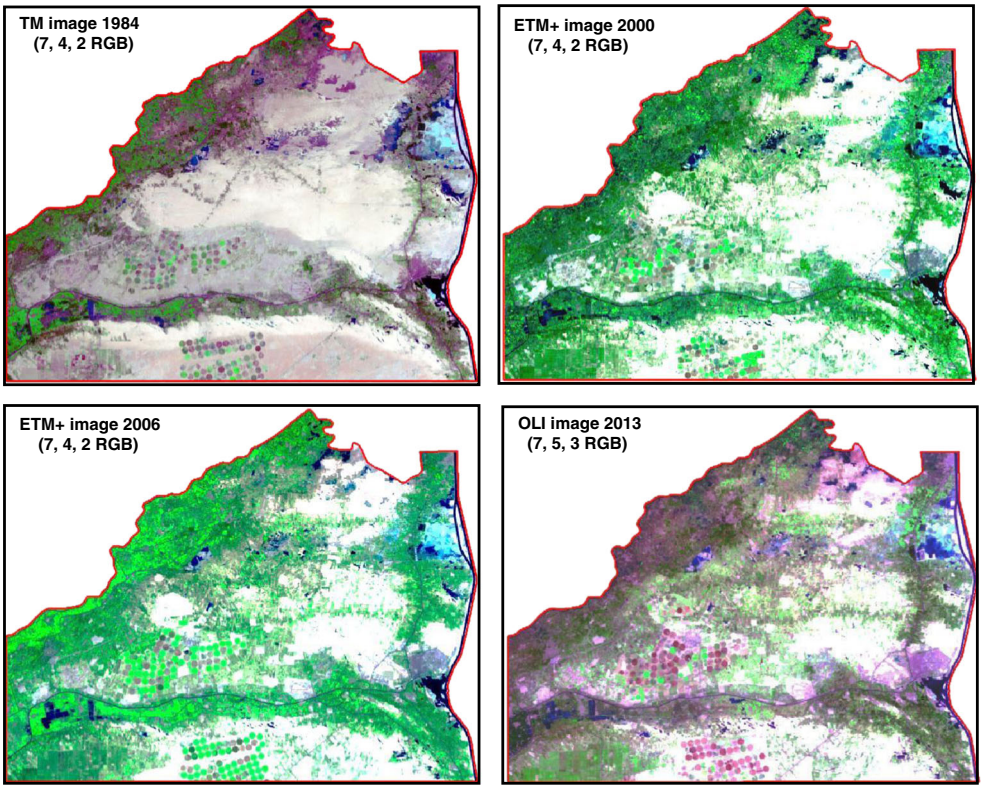

Fig. 2 Multi-temporal landsat satellite images sets (1984–2013) that are used for conducting image processing

waterlogging and salt-affected hazard vulnerabilities of the study area. Primary and secondary data were converted into digital layers and then overlayed and integrated to construct the thematic and change detection maps. The thematic information was prepared using enhanced RS images, geo-referenced and other ancillary data - such as the attributes of point, line and polygon coverages - and a database.

Analysis, results and discussion

Digital image processing and analyses

Satellite RS data, coupled with a GIS, offers an excellent alternative to conventional mapping techniques previously used for monitoring, assessing and deriving environmental degradation hazard maps. The advantages of using RS technology include: time savings, as wider coverage is faster than any ground-based survey methods, and facilitates long-term repeat monitoring. Satellite techniques provide multi-spectral and multi-temporal images with resolutions that range from medium to high such as landsat series, as well as hyperspectral imagery.

Digital image processing plays a significant role in providing geo-information in a standard spatial format and also for determining, enhancing and monitoring the overall capacity of the Earth. In the present study, digital image processing methods were used to enhance multi-temporal Landsat images and to produce various thematic maps. Remote Sensing methods to identify the best results for monitoring and assessing wasteland areas and the environmental impact hazard indicators include the selection of optimal bands of spectral reflectance for comparison with other spectral wavelengths. In addition, optimal digital image processing techniques are used to delineate, evaluate and map the temporal RS data results. Spectral response patterns - using multi-temporal and multi-spectral measurements - of various terrain features are necessary to collect primary information on LC and the environmental degradation indicators of waterlogging and salt-affected soils. Moreover, the spectral response patterns for saline soils are extremely useful as they help in the segregation of salt-affected soils from waterlogged, normal soils, poorly drained soil, urban, bare land, and vegetation LC classes. The amount of reflected solar radiation varies with wavelength which is based on the physical and chemical compositions of the discrete types of LC, which affect the possibility of identifying various kinds of LC surfaces or classes in RS data and to discriminate between them using the differences in reflectance. To generate spectral response curves of the various selected major classes, RS data were displayed and spectrally homogenous areas representing various categories were then visual identified. Seven major classes were separated. These were vegetation, salt-affected, waterlogged, urban, saline poorly drained soils areas, and in addition, water bodies like lakes, canals and drains for irrigation for relative comparison. Spectral responses in different spectral bands in the form

of reflectance values were produced for various LC surface classes. Furthermore, a field survey was undertaken of these training sites for the LC classes to help to establish the causes of wasteland arising from waterlogging and salinity indicators. The training sites for waterlogged and salt-affected indicator areas, which have a relatively lower and higher reflectance coefficient in the spectral bands of RS data, were selected from multi-temporal RS images taking into account all of the surface information collected. The spectral response curves for all the classes at the selected training sites are shown in Fig. 3. Using the reflectance values, and confirmed by the results of (Metternichit and Zinck 1997; and Khan, et al. 2005) where spectral pattern variation for the training classes of waterlogged, salt-affected, vegetation, urban and bare land areas were recorded for all images and for all bands and then normalized to near infra-red (NIR) band to provide a visual comparison of variation with time and each band for that particular class. It was also found that salt-affected land had high spectral reflectance in the visible spectrum, particularly in the blue and red range of the spectrum at low moisture content. There is also a possibility that the spectral data could have been affected by certain external effects such as soil moisture and atmospheric factors. The results also indicate that the spectral response pattern of salt-affected land is higher than for the other classes in all bands and in all images. This is in addition to the fact that salt-affected soils that have been found to reflect more incident light energy in the visible spectrum than those of other LC features, whereas vegetation reflects maximum values in the NIR range. These results showed that there is a noticeable variation with time in each band response for that class which could be attributed to a change in LC, vegetation canopy and atmospheric parameters such as temperature, moisture, and density (also precipitable water, clouds, aerosols etc.). Therefore, it can be concluded that time has an important role to play in information extraction and the detection of certain classes.

Environmental impact hazards of the study area can be identified by applying a contrast stretch of the optimal band combination, PCA, classification techniques, and in addition using the NDVI, NDWI, NDSI, and NDBI indices. The enhanced contrast stretched images of the best band combination (7, 4, 2 RGB) for TM and ETM and (7, 5, 3 RGB) of Landsat 8 was successful for discriminating the waterlogged and salt-affected areas for the visual interpretation (Fig. 2). Waterlogged areas appear very clearly as a dark blue to bluish black tone or bluish black to light bluish tone and various shades of blue, that are confined to local depressions on either side of canal courses and gentle slopes. Salt-affected soils can be identified by their dull-to bright-white and cyan colour.

Indices combine two or more spectral bands and have been widely acknowledged as powerful tools for identifying features of interest. Many studies describe a wide range of band combination/indices developed for vegetation vigor, crop assessment and LU/LC changes. However, there is scarcity of information about the ideal band combinations for waterlogged and salt-affected lands (Khan et al. 2005). Some band combinations are potentially useful to discriminate salt-affected and water bodies/waterlogged areas. The bands used were selected after examining the spectral reflectance curves of the multi-temporal RS data for the study area, in addition to a review of relevant literature. Five important indices were applied to detect, identify, monitor and assess the waterlogged and salt-affected areas and their major environmental degradation causes.

Due to absorption in the visible range and high reflectance in the NIR range of the electromagnetic spectrum, NDVI has

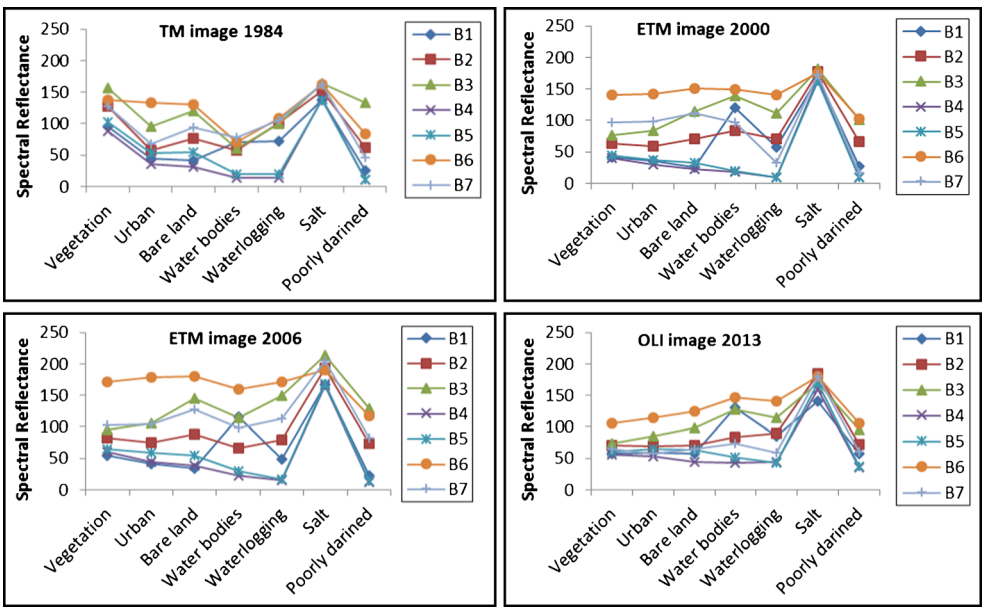

Fig. 3 Showing the spectral response pattern curves for various land cover classes of the multi-temporal landsat data

been widely used for vegetation mapping (Deering and Rouse 1975; Fernandez-Buces, et al. 2006; Jabbar and Chen 2008; Elnaggar and Noller 2009). The most common form of vegetation index is the Normalized Difference Vegetation Index or NDVI (Purevdorj, et al. 1998). NDVI is the difference between the red and near-infrared band combination divided by the sum of the red and near-infrared band combination or: $NDVI=(NIR - R) / (NIR+R)$ where R and NIR are the red and near-infrared bands. This normalizes the differences in the amount of incoming light and produces a number from -1 to 1; the range of actual values is approximately 0.1 for bare soils to 0.9 for healthy vegetation. By comparison with the enhanced NDVI for an image for 29 year timespan (Fig. 4), there is a high increase in the vegetation cover and land reclamation in most of the investigated area which is intensively cultivated and mostly irrigated, whereas, there is a decrease in the bare land and appear waterlogged and salinization effects of soils with patchy vegetation

There are also problems with land degradation in an arid environment such as waterlogging, wetlands and inadequate irrigated agriculture system. The NDWI is used to estimate the spatial extent of surface waterlogging in the investigated area. The NDWI was developed to delineate open water features. $NDWI=(band\,4-band5) / (band\,4+band5)$, where $band4$ and $band5$ represent the spectral bands of the Landsat TM and ETM+ images (Mcffers 1996). In the current study the $NDWI=[(band5)-(band6)] / [(band5)+(band6)]$; where ($band5$ and $band6$) of the Landsat 8 image. The analysis of the enhanced NDWI images shows that the values of NDWI for irrigation and drains channel pixels are close to 0, being more than 0.3 for lakes and waterlogged areas. The NDWI value for surface waterlogged areas identified in the multi-temporal RS data is fixed in pixels values**.** The results from the enhanced NDWI images reveal a significant decreases and/or increases in area coverage of water bodies over the timespan of 29 years (Fig. 5). The area of water bodies shows a positive change due to the addition of reservoirs, the construction of irrigation canals, drains and new farms established in recent years which are the result of extensive human agricultural activities, mostly relating to irrigation. In irrigated areas, farmers may not be able to control irrigation that commonly results in excess water being added to the groundwater. Continued irrigation for further agricultural activities and reclaiming new lands with excess water induces a rise in the groundwater table. Waterlogging of low-lying areas is created by the seepage of water from irrigated uplands and from the canal system. In areas of excess irrigation near Ismailia, Port-Said and Suez Canal water, it is needed to apply water management practices to culminate the waterlogging. This is due to the flooding of many agricultural lands, additional infrastructure, houses, industrial zones and electricity towers as well as accessibility from railways and roads in some areas (Fig. 6).

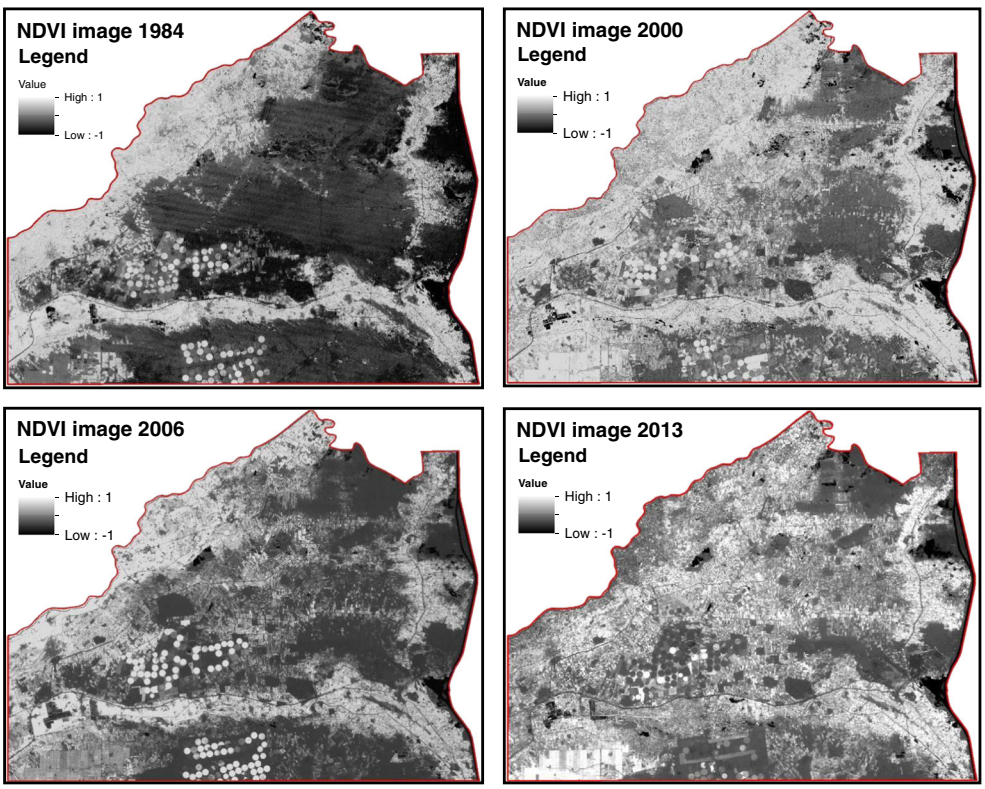

Fig. 4 NDVI enhanced multi-temporal landsat images of the study area; showing the change of vegetation covers, land reclamation and waterlogged areas

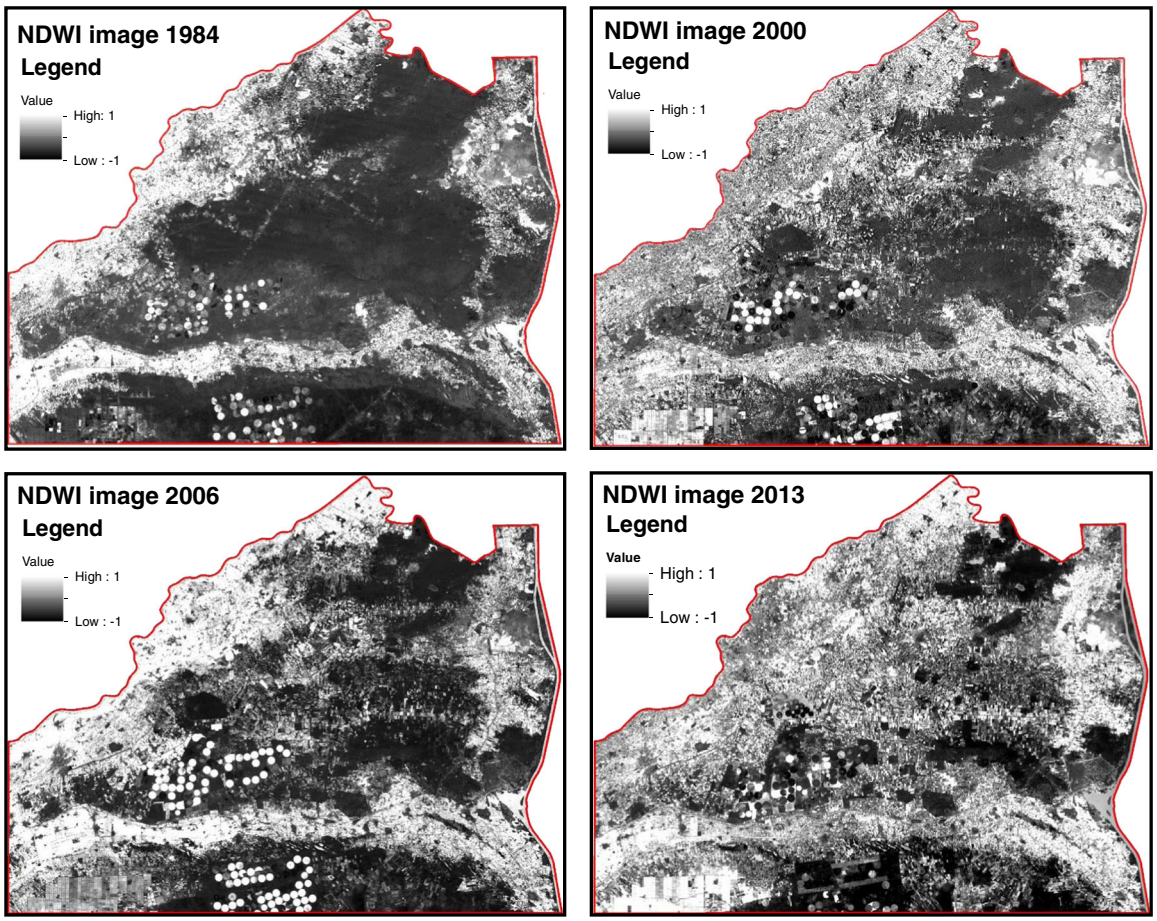

Fig. 5 NDWI enhanced multi-temporal landsat images of the study area; showing the change of distribution of wetlands and water bodies

Multispectral RS data have been the preferred method for monitoring, assessing and the mapping of wastelands. Salinization and waterlogging have long caused serious damage to the land in arid and semi-arid regions in the world. However, the agricultural activities and land reclamation projects, and moreover the misuse of the water resources (groundwater and surface water) have been the main reasons for secondary salinization in the study area. The NDSI is the reverse of the NDVI index for vegetation (Tripathi et al. 1997). It is basically the difference between the red and near-infrared band combination divided by the sum of the red and near-infrared band combination, or the algorithm used was: NDSI = [(band3) − (band4)] / [(band3) + (band4)], where band3 and band4 represent the spectral bands of the Landsat TM and ETM+ images. While the algorithm for Landsat 8 images is: NDSI = [(band4) − (band5)] / [(band4) + (band5)]. The resulting enhanced NDSI images (Fig. 7) show an increase in the effects of salinity from 1984 until 2013. In addition, there is some similarity between the salt-affected areas and urban areas observed in the current study. This indicates that multispectral RS data sometimes - owing to the time of the data acquisition – leads to reflectance confusion as a result, and non-saline soils can be confused with bare land (Furby 1995). In the present study, these results were confirmed by Khan et al. (2005) and urban sites were shown to have the same or similar spectral signature to that of salt-affected areas. This may be down to the existence of muddy rooves in the settlement areas that are similar in appearance to dry barren soils along with patchy areas in the study area. The main difficulty in the retrieval of salt-affected areas from RS data lies in being able to distinguish between the saline and urban classes. To overcome this problem, urban areas can be vectorized using GIS tools and then excluded or masked from the calculation of surface changes when monitoring the salt-affected areas. Moreover, the problem can be established by selecting RS data for the optimal time period to assess the salt-affected areas by applying the NDVI index in the spring season, particularly in March, to avoid confusion with urban areas that happens in the peak summer season.

To extract urban land from the Landsat imagery, a new index (NDBI) (Zhao and Chen 2005) was used in this study that is sensitive to the existence of built-up areas. NDBI was devised by analyzing the spectral characteristics of different LU /LC classes: $NDBI = [(band5) - (band4)] / [(band5) + (band4)]$, where *bands* (*band*4 and *band*5) of the Landsat TM or ETM+ images, and also, in the current study the *NDBI*

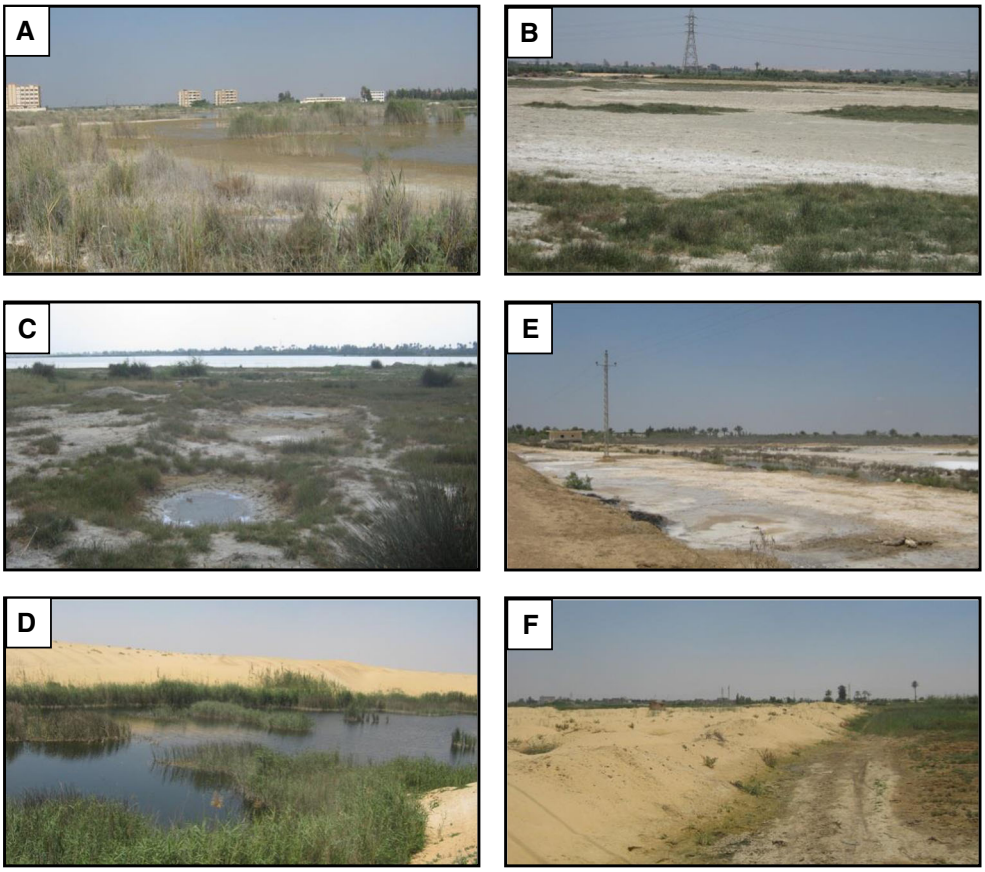

Fig. 6 Showing the waterlogged and salt affected areas; Waterlogged areas viewing in (**a**) at El-Ballah, (**b**) at Barket Mehasher and (**c**) at Wadi El-Tumilat micro-depression between sand dunes. While (**d**) at Abu Suwir and (**e**) at El-Salhyia road areas showing the salt encrustation and unsaturated saline soils in agricultural land. (**f**) Indicating the human activities for reducing the waste agricultural lands at El-Mahsama by covering the waterlogged and saline soil by sand sheet

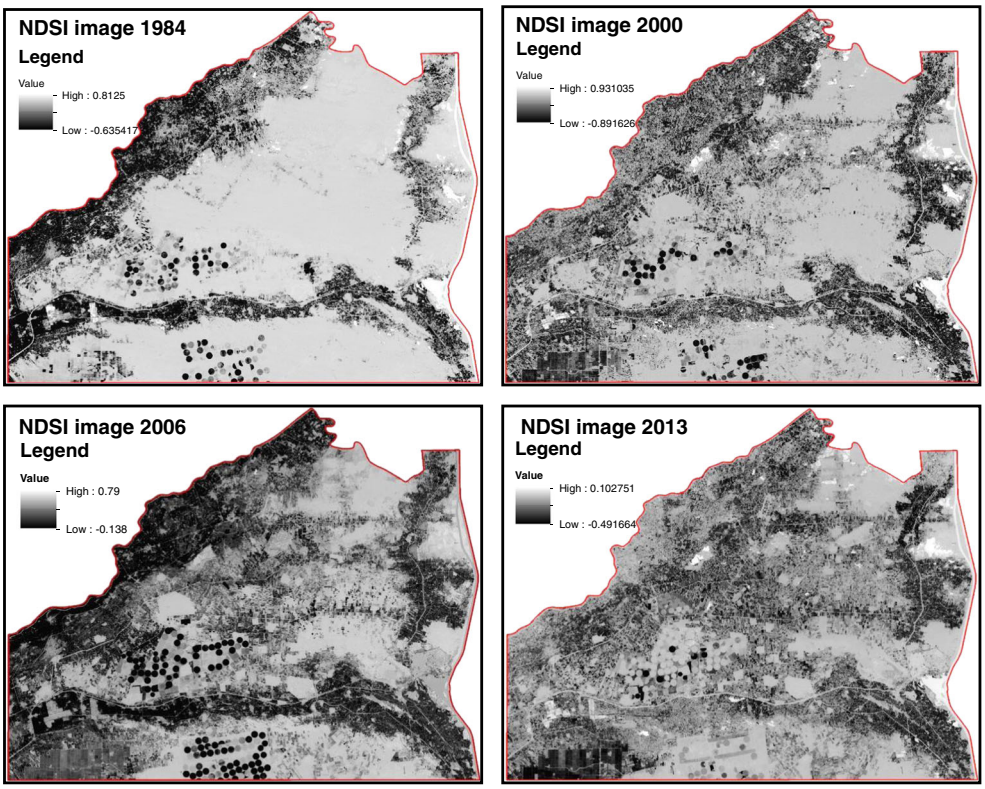

Fig. 7 NDSI enhanced multi-temporal landsat images of the study area; showing the change of salt-affected and waterlogged areas distribution

= [(*band*6) − (*band*5)] / [(*band*6) + (*band*5)]; where (*band*5 and *band*6) of Landsat 8 image. Analysis of the urban boundaries (cites and settlements areas) using the NDBI index and multi-temporal images reveals that the study area has undergone a rapid urban expansion from 1984 to 2013. The causes of urban expansion are related to the increasing population and the sustainable development project established in the last three decades for agricultural, economic, and technological development.

Principal Components Analysis (PCA) is often used as a method for data compression. It allows redundant data to be compacted into fewer bands; that is, the dimensionality of the dataset is reduced. The bands of PCA data are non-correlated and independent, and are often easier to interpret than the source data (Faust 1989; Jensen 2004). The PCA approach is applied to monitor, delineate and assess the waterlogged and salt-affected areas from the multi-temporal Landsat data used in this present study. PCA is carried out based on the mean, standard deviation, correlation coefficient and variance / covariance matrices to analyse the multi-temporal RS images and to produce new images that are uncorrelated with each other and to account for progressively less variance found in the original set of spectral bands. The PCA images generated have the highest covariance load values of PC1, PC2 and PC3 respectively and reveal the different LU/LC classes in the investigated area (Fig. 8). These results from PCA provide the current study with clear results concerning the salt-affected, permanent, temporal waterlogged areas and water bodies. Moreover; PCA techniques provide the means to discriminate the urban, vegetation, bare land and saturated saline soils. PCA is therefore a promising potential technique for delineating the hydrosalinized wastelands.

Finally, field verification was carried out to check the interpreted images and to determine the main causes for the land degradation through waterlogging and salinity. Local farmers were also interviewed about water table depths, salinity problems, villages under water logging, canal seepage, cropping pattern and other possible reasons for waterlogging and salinity in the area.

Monitoring and assessment of waterlogged and salt affected hotspot mapping

Visual interpretation based on satellite image characteristics, and a prior knowledge of the study area from the field verification and other published ancillary data, was carried out to delineate waterlogged and salt-affected soils areas (Fig. 9). The multi-temporal RS images were considered as a base map for the delineation of different wasteland classes, where separation amongst LU / LC classes is clearer in the months of September and October. This helped in the improved identification and mapping of wastelands. An area is said to be waterlogged when the water table rises to an extent that the soil pores in the root zone of a crop become saturated, resulting in the restriction of the normal circulation of air, decline in the level of oxygen and increase in the level of CO2 (Anonymous

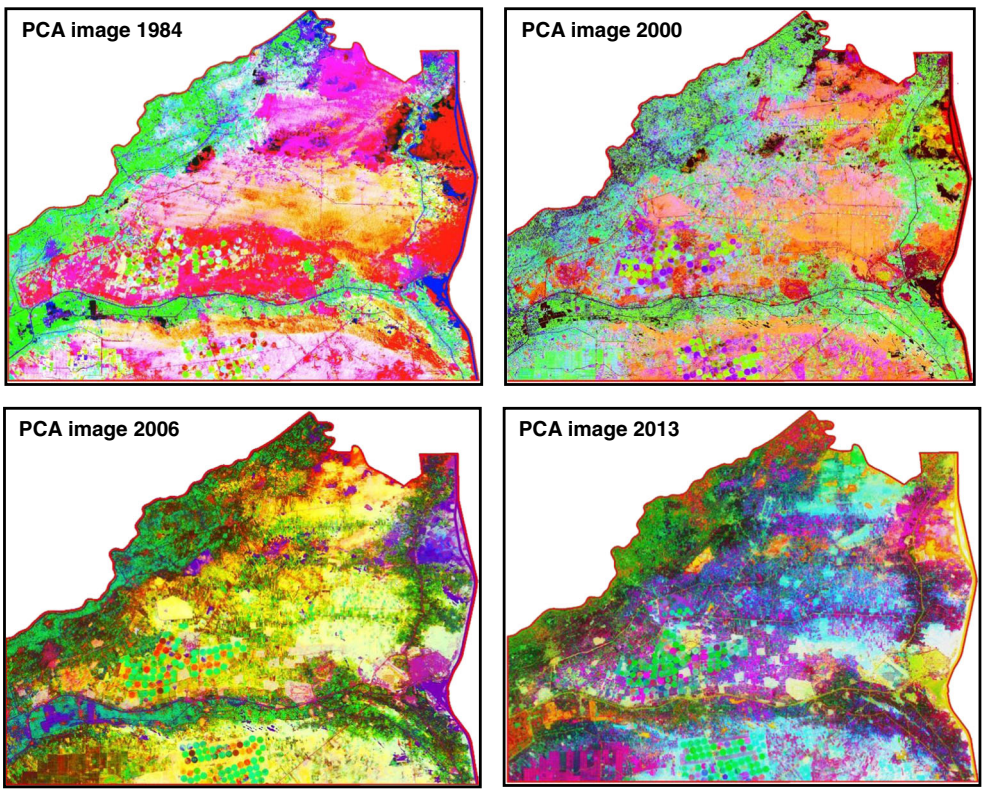

Fig. 8 PCA enhanced multi-temporal landsat images of the study area display composite of PC1, PC2 and PC3 as RGB; showing the change of the LU/LC classes

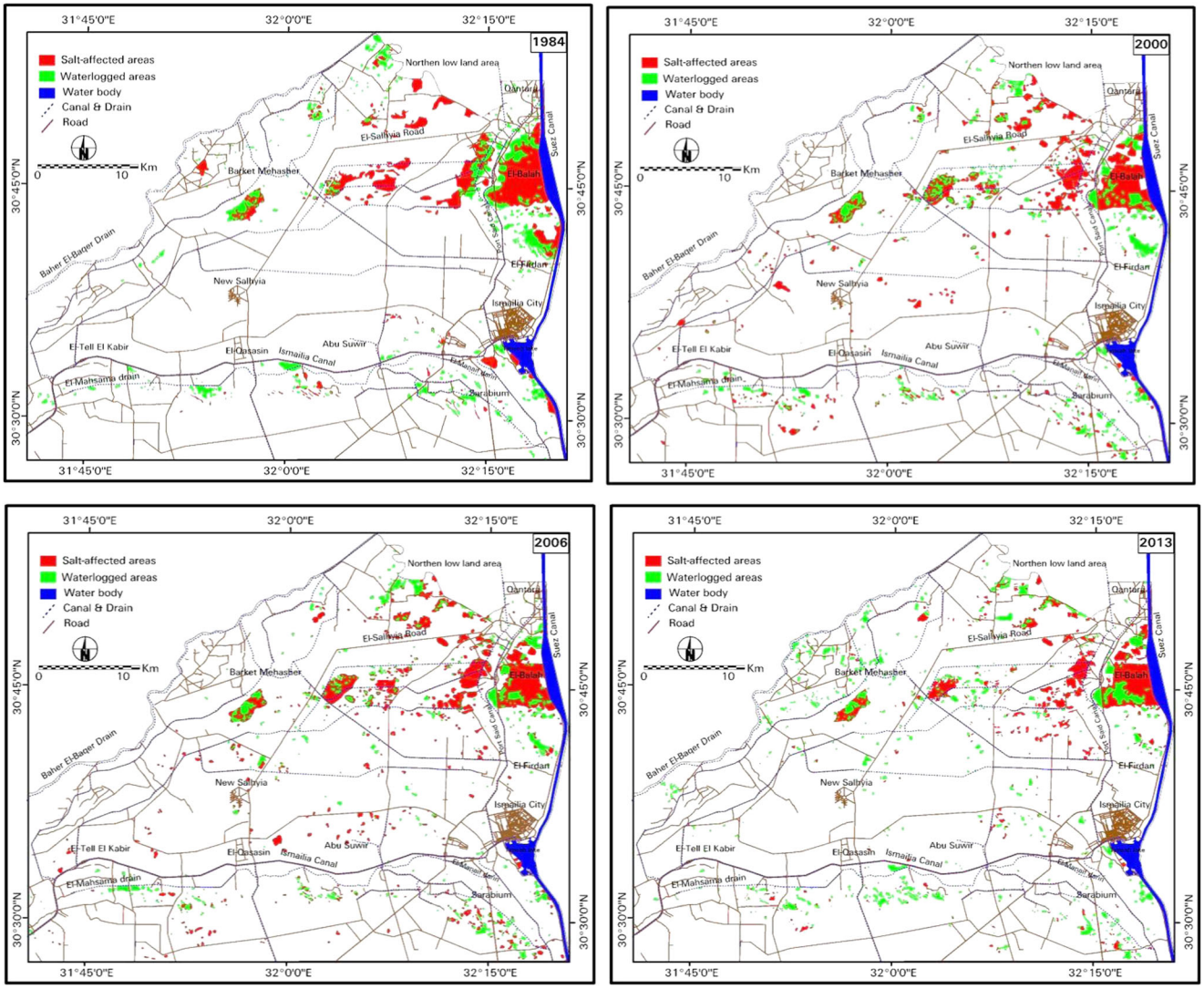

Fig. 9 Multi-temporal spatial distribution maps from 1984 to 2013; showing the waterlogged and salt-affected areas distributions in the study area

1976). Surface waterlogged areas and water bodies exhibit similar reflectance characteristics, which can be discriminated from other associated land covers like salt affected soils, water bodies, fallow land and croplands by virtue of the very low spectral response in all the spectral bands, especially in the near infrared (Dwivedi and Sreenivas 1998a, 1998b). To determine the waterlogging dynamics visual interpretation of the enhanced multi-temporal Landsat images was used then to identify, delineate and integrated using ArcGIS. The multi-temporal and multi-spectral Landsat images of the study area were used for image processing and to carry out mapping of the spatial distribution of the dynamic change in waterlogging and salt-affected soils spanning 29 years from 1984 to 2013. Based on the best visual interpretation of the enhanced PCA Landsat images of the investigated study area reveals the wasteland classes arising from waterlogging and salt (Fig. 10).

The multi-temporal hotspot waterlogging and salt-affected soils of the study area are mapped based on the visual interpretation of the enhanced RS images and the field observations by using ERDAS Imagine and ArcGIS software; the results of hotspot delineation are represented in Fig. 9. The multi-temporal hotspot maps show the change in the extent and spatial distribution within the time span of the satellite images due to the natural and / or human activities particularly the agriculture and urban activities. The water logged areas were categorized into permanent water, temporary "Seasonal" water and sensitive waterlogged areas. An area, which remains waterlogged throughout the entire year, is termed a permanent waterlogged area, and the remaining waterlogged areas, which generally dry up before the end of the spring cropping season - ending by the middle of April – are termed as temporal waterlogged areas. In addition, the areas that appear and disappear from time to time are considered as sensitive waterlogged areas. According to the acquired RS data in the present study, the seasonal waterlogged areas appears very clear in different shades of blue and cyan in the standard false

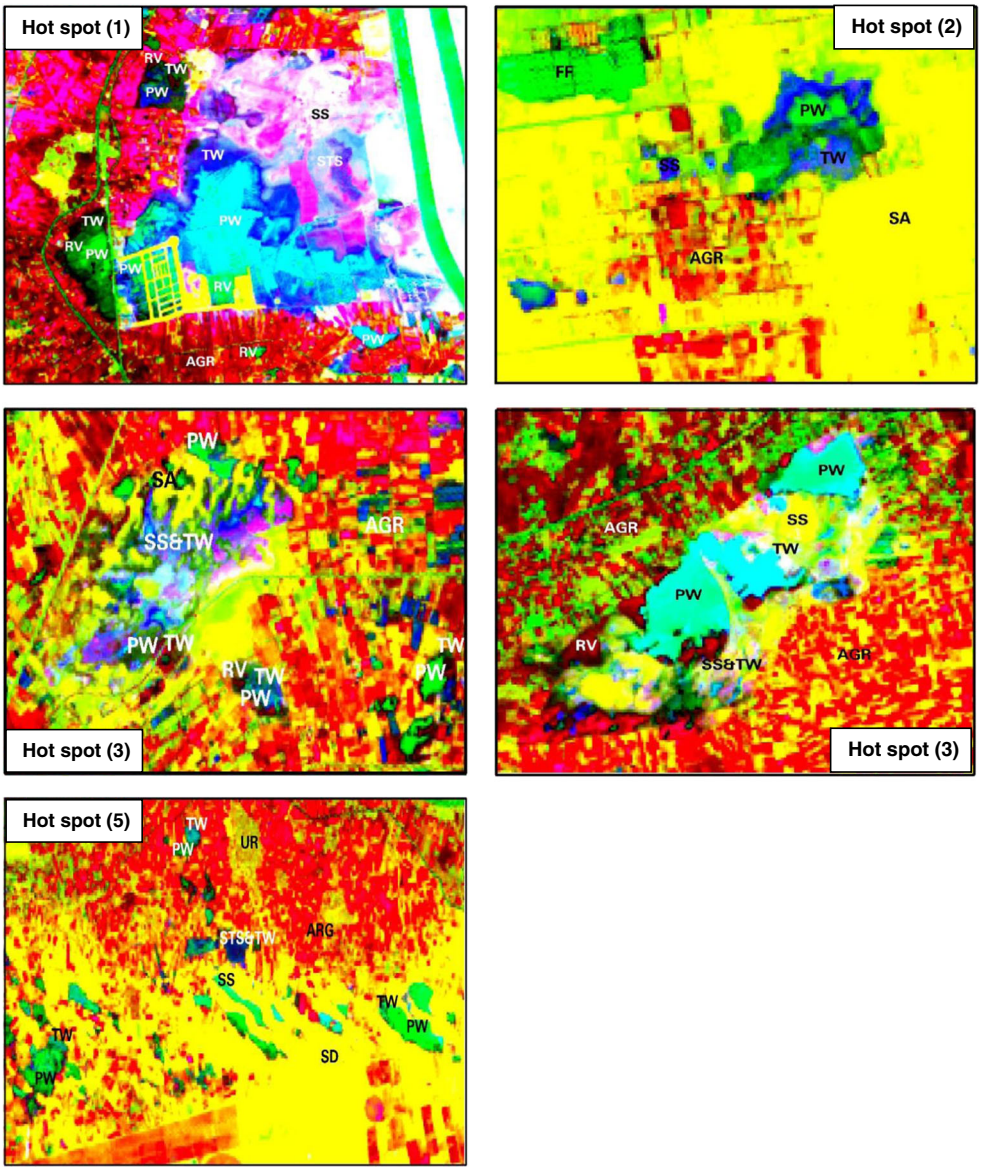

Fig. 10 PCA enhanced subset images of the hot spot areas in the study area showing the different indicators of the wastelands; where permanent waterlogged (PW), temporary waterlogged (TW), agricultural (AGR), reed vegetation (RV), saline soil (SS), sand (SA), sand dunes (SD), urban (UR), saturated saline soil (STS), saline soil and temporary waterlogged (SS&TW) and fish farms (FF)

colour composite images produced from RS multispectral data, and acquired during the months November and December (Dwivedi et al. 1999).

To identify and estimate the dynamic change in the waterlogged and salt-affected soils several ArcGIS functions were used. The results of the integration of these layers (Fig. 9) reveals that 11.40 and 76.93 Km^2 of area are affected by seasonal and permanent waterlogging respectively. Moreover, 85.20 Km^2 areas are saline soil (dry saline or saturated saline soils) from 1984 to 2013 respectively. A reduction of 173.53 Km^2 wasteland area especially in classes like permanent and temporary waterlogged are identify and delineated in multi-temporal vector layers (Fig. 11).

Trends and rates in the extent and change of the waterlogged areas were determined quantitatively by a comparison of the statistical results of the change detection enhanced images of the total area separately in the years 2013, 2006, 2000 and 1984 where the salt-affected soils occur near the water bodies. With the change in the size of the waterlogged areas, some of the soils near water bodies were exposed and salt affected in new area but they were also under water with the increase in precipitation. The areas and their percentages of the total area are increasing year by year and are accelerating. These changes in the conditions of the wasteland were described visually using the change detection maps (Fig. 12). The positive changes shown in a red colour are those that occurred in the final state and not in the initial state, while the negative changes in green colour are those that take place in the initial state and not in the final state. In addition, the results of change detection of the waterlogged areas during years 1984–2013 indicate that its surface area increased around 28.30 Km^2 and decreased by about 29.33 Km^2

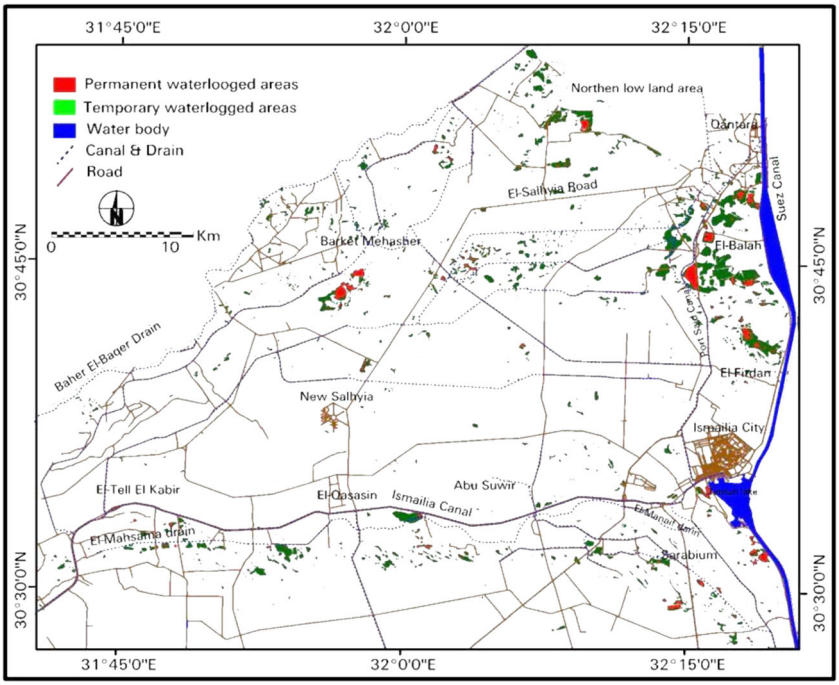

Fig. 11 showing the spatial distribution of permanent and temporary waterlogged areas in the study area

(Fig. 12). At the same time, the salt-affected surface areas increased by about 50.38 Km^2 and decreased by about 44.94 Km^2 (Table 1). In addition, a fairly large area is occupied by waterlogging during October. Over time, the outer boundaries of such waterlogged areas dry up due to natural salinization, and only the central portion remains waterlogged until the end of April. During the month of May salt has accumulated on the surface due to increasing evaporation rates, in addition to the human activities that are may be due to secondary soil salinization in the study area.

According to the statistical results in Table 2 and the field verification, the main reasons for the fluctuations in the statistical calculations of waterlogged and salt-affected areas over 29 years are due to the human activities used to overcome these problems. There are four human activities represented in the study area where the most urban communities and villages work in activities of land reclamation, fish breeding farms and industry. According to these activities the land reclamation - especially washing salt-affected lands – has transformed about 12.80 and 17.26 km^2 from the waterlogged and saline soils respectively to fish breeding farms in the north, northwest along the El-Salhyia road and along the Suez canal in the northeastern sites. These indicate that the surface areas of waterlogging and soil salinization have changed with a rate +0.32 and −0.32 Km^2/year respectively. Furthermore; the local farmers covered many of the sites with sand and agricultural fertilizers and also, drained the waterlogged water into the agricultural drains particularly along Wadi El-Tumilat and Ismailia fresh water Canal. Moreover, the government have constructed many wastewater treatment plants within the study area in and around the waterlogged and salt-affected areas and also the urban and settlement areas. All of these areas have been observed in the enhanced satellite images but are excluded from the statistical calculations of the waste-land area.

Terrain analyses for landforms, susceptibility waterlogging and salt-affected mapping

From the geomorphological point of view, the problems of waterlogging and salt are further compounded by natural factors such as the existence of low-lying areas, topographic depressions, buried paleo-channels, the absence of natural drainage. These factors create an increase and / or decrease in the size and extension of these problems particularly with many associated hydrogeological conditions and network irrigation systems. In the current study, using ASTER GDEM and topographic map analysis to investigate the topographic situation of the study area, it is appeared that there is a difference in altitude between the southern and the northern hotspot waterlogged areas which lead to land degradation. According to field verification (Geriesh 1994; Mansour 2012; and Kaiser, et al. 2013) there is an impeded clay layer in the south of the study area located at a much greater depth in areas where waterlogging is present particularly along the south Wadi El-Tumilat. Also, the higher topographical location of these waterlogged areas can be found on topographical maps. But, the waterlogging and salt- affected soil areas are directly connected to the absolute height of the landscape (Fig. 13). Five topographical levels of waterlogging can be distinguished by applying slicing techniques to the GDEM. Based on several controlling factors for mapping such as the results of enhanced

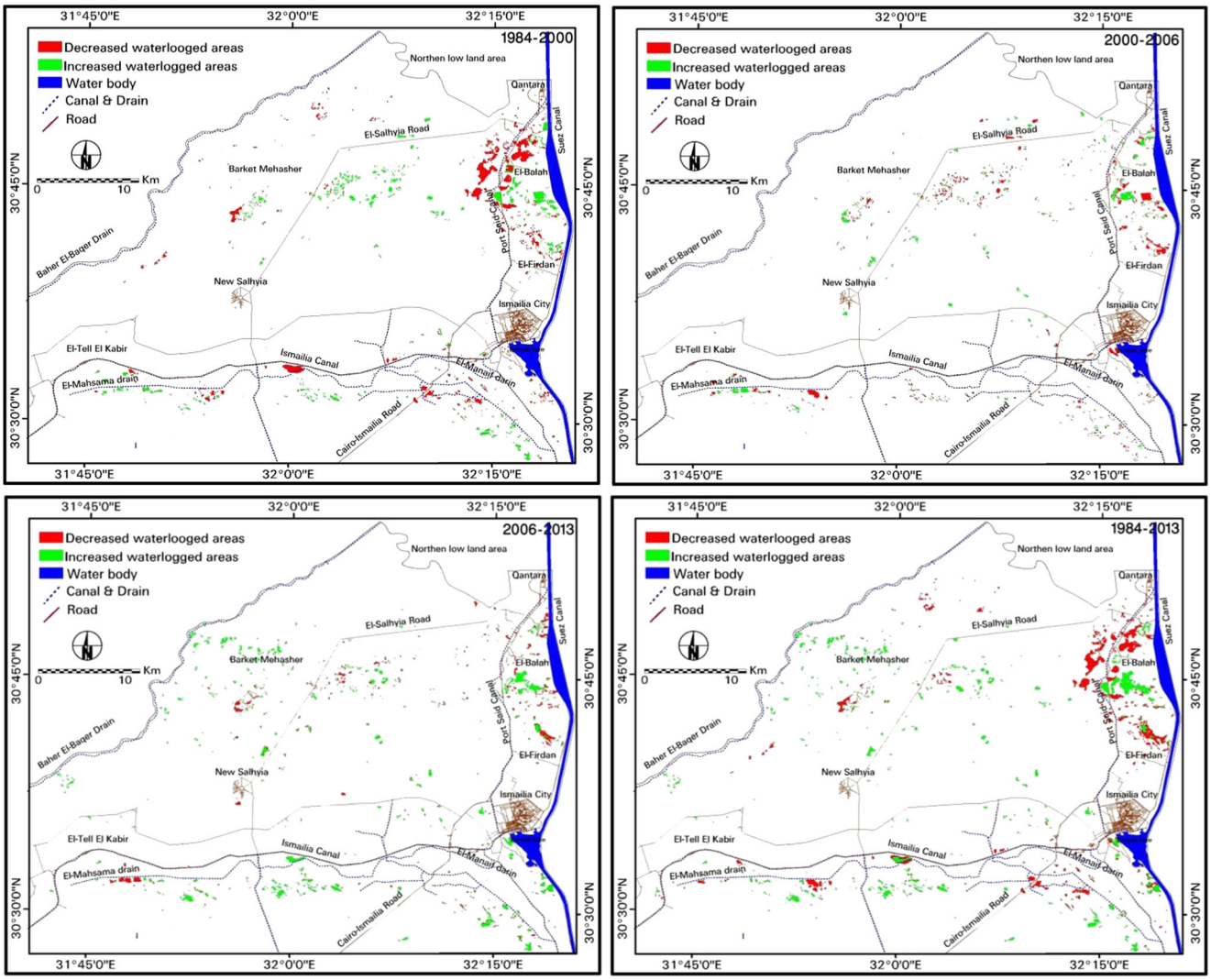

Fig. 12 Change detection of the multi-temporal spatial distribution maps of waterlogged and salt-affected areas from 1984 to 2013 in the study area

RS data; geomorphological and field verification data, depth to groundwater and rising of the groundwater table to be indicate areas that may be become waterlogged and then salt-affected occurs (Fig. 14). The difference in the altitude of waterlogging areas is not sufficient on its own but must be integrated with the flat slope of the study area by using GIS tools to eliminate any areas that have a high probability of forming waterlogged areas.

According to the integrated depth to groundwater, slope and elevation parameters, and subsequently confirmed by field work and other ancillary geological and hydrogeological data in (Fig. 15), hotspot area one (−1–3 m a.s.l.) are located in the north, in the low land area of the Isthmus stretch and along the Ismailia-Qantara road. All soils are waterlogged and saline. Furthermore, gypsiferous soils occur in the waterlogged areas in the east particularly in El-Ballah and near to El-Qantara areas where the soluble and non-soluble salts occur by a series of salty lakes related negative altitudes. Moreover, the saline soils in this area are located in the south Timsah Lake and south west of the Suez Canal. Also, this zone is

Table 1 Showing the increased and decreased areas based on the change detection calculations with timespan 29 years

Period	Feature	Decreased (Km^2)	Increased (Km^2)	Feature	Decreased (Km^2)	Increased (Km^2)	Span time (Year)
1984–2000	Waterlogging areas	25.80	18.30	Salt-affected areas	42.07	69.75	16
2000–2006		14.82	10.33		22.21	25.38	6
2006–2013		11.71	23.82		27.18	20.50	7
1984–2013		29.33	28.30		44.94	50.38	29

Table 2 Showing the areas and their rate of change for waterlogged and salt-affected areas from 1984 to 2013

	Waterlogged area (Km^2)	Salt-affected area (Km^2)	Rate of waterlogging change (Km^2/year)	Rate of salt-affected change (Km^2/year)
1984	42.23	104.61	–	–
2000	34.52	77.11	−0.48	−1.72
2006	31.39	80.91	−0.52	+0.64
2013	38.68	78.10	+1.04	−0.41
1984–2013	51.48	95.36	+0.32	−0.32

considered to be most critical susceptible waterlogged area. In addition, within this level (hotspot two 1–3), there is no reed vegetation and the high salinity in the north-east is located provide an indication of saline and poorly drained soils. Furthermore; this zone ranges between most critical to critical susceptible waterlogged area. The majority of this area is being transformed into fish farms with a few agricultural activities within the timeframe of 29 years. Hotspot area three - the waterlogged area at an altitude between 1 and 4 m a.s.l. - is located mainly along the Ismailia-Salhyia road and Barket Mehasher in the east. It is vast area of waterlogged and strong saline soils which are poorly drained - particularly in the past - and is covered by evaporitic loamy sand, sand and sand dunes, and in addition by Nile silt and mud near Barket Mehasher. This zone is classified into the most critical susceptible waterlogged area located to the north east while the critical area located at Barket Mehasher and the rest of zone is not critical. Today, this area is affected by a major project to reclaim the saline soil for sustainable agricultural and irrigation developments. Hotspot area four (6–8 m a.s.l. level) is located in the El-Salhyia plain and extends from west Ismailia to New Salhyia cites and is also covered by gravely sand, sand and sand dunes. The agricultural development usually increases over time and land reclamation is fully operational as well as the irrigation of the area. The soil is slightly saline and the local farmers do misuse irrigation by using flood irrigation methods leading to waterlogging and secondary soil salinization. In the last two decades to the west of Ismailia city there have been more urban, industrial and agricultural activities that, together with the existence of the waterlogged and salt-affected problems, also threaten the sustainable development in this area. Where the water table is rising over time and show as waterlogged in lowland geomorphological areas. Generally, this zone is classified as not critical susceptible waterlogged except some localities nearest to Ismailia city at El-Mostakbal and the industrial zone area while the rest of zone is not critical.

Hotspot area five, at an altitude more than 6 m a.s.l., is covered by Nile silt, mud, sand dunes and gravely sand of the Wadi El-Tumilat depression and Um Gidam slopes. This hotspot area extends from Sarabium and El-Manaif in the east to El-Abassa and Tell El-Kabir in the west. This hotspot is

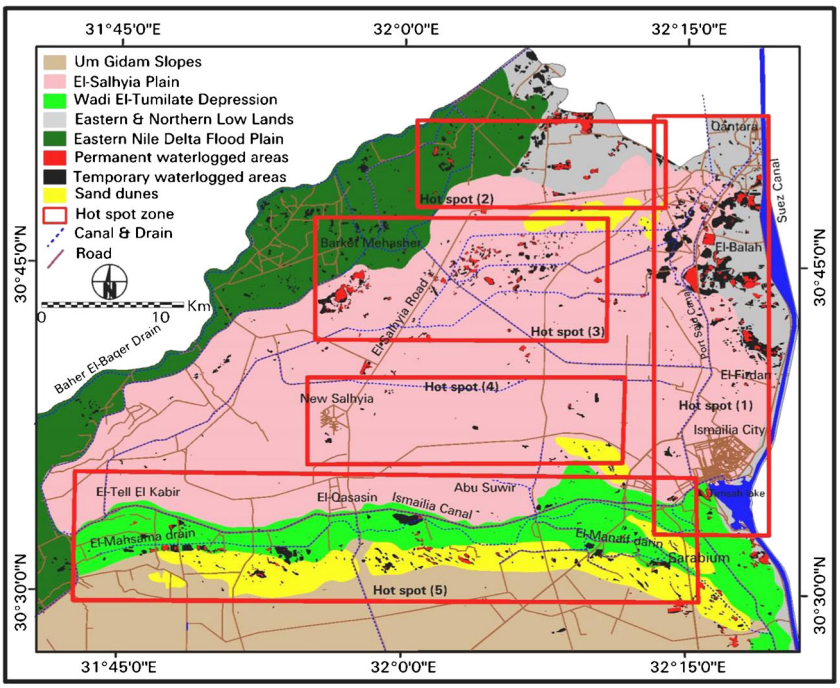

Fig. 13 Showing the landform units those are extracted from the enhanced RS data and other ancillary data; then overlaid by the surface waterlogged and hot spot areas of the study area

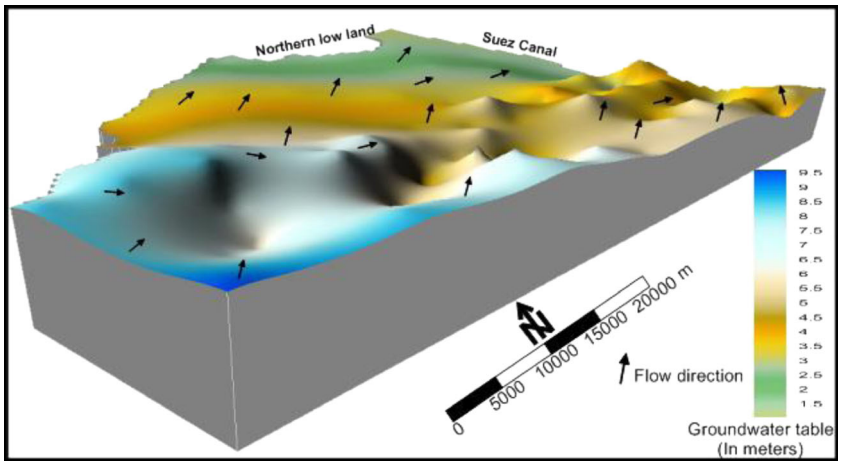

Fig. 14 3D view map created from the groundwater table measurements of the study area

different from the previously mentioned hotspots; where there are two waterlogging classes between 5 to 6 and 6 to 7 m a.s.l. Also most of the waterlogged areas are situated in micro-depressions in the Wadi El-Tumilat. The flat areas correspond to depressions that are surrounded by undulating sand dunes. These are considered potential risk zones for waterlogging and soil salinity. In addition, the western part of this hotspot suffers from waterlogging and soil salinity with dense agricultural activities and scant vegetation with drip irrigation in the southern middle part of the Um Gidam slopes. This zone has three sites: one in the west around the El-Mahsama drain reveals an anomaly for the most critical and critical susceptible waterlogged area; in the middle the areas are less crucial. In addition, at the east south of El-Manaif drain and Sarabium are classified as critical to less critical susceptible waterlogged areas while and the rest of the zone are not critical.

Change detection of land-use / land-cover environmental indicators maps

RS data and GIS offers an excellent alternative to conventional mapping techniques in monitoring and mapping of wasteland areas. One of the most sustainable development projects in Egypt has been carried out in the eastern Delta, especially the agricultural developments along and around the desert fringes. Variations in the LU/LC along the study area investigated have been identified through the analysis of multi-temporal satellite images with the aid of GIS analysis. Jensen (2004) describes various change detection analysis methods that can be used to perform change detection of multi-date RS data. In this study the band differencing technique was applied in particular with normalized band 4 over a time period of 29 years (Fig. 16). As stated by Jensen (2004), a change image

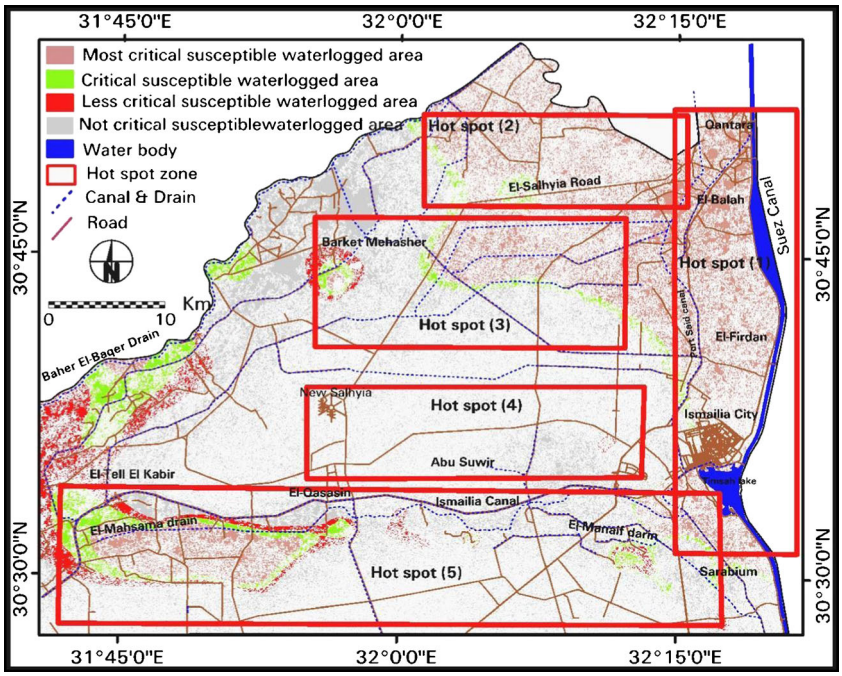

Fig. 15 An integrated susceptibility waterlogging risk map of the study area based on depth to groundwater, slope and altitude topographic digital maps

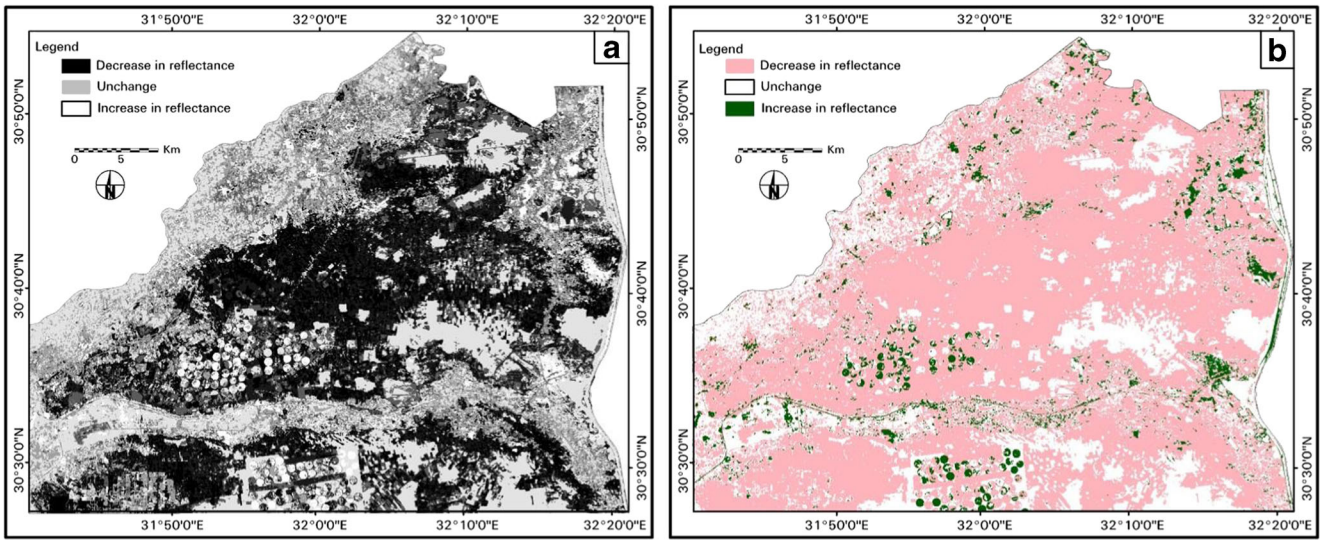

Fig. 16 Difference image (**a**) show that, grey colour indicates no or minor changes; while extreme dark and *white pixels colour* indicate changes. While the recoded image (**b**) that is draped on the top of difference image to show the increase and decrease in reflectance of the study area in dark green and pink colour respectively

produced using image differencing usually yields a DN distribution that is approximately Gaussian in nature, where pixels of no DN change are distributed around the mean and pixels of change are found in the tails of the distribution. This has been evident in the current study and Fig. 16a shows the resulting distribution of the difference image. The image is created in a signed 8-bit file type and stretched for display to a gray scale of 0-255 range. The extreme decreased reflectance pixels are displayed in black (1631 Km^2), and extreme increased reflectance pixels are displayed in white (122 Km^2). Values in between are displayed as grey, while Fig. 16b reveals the recoded image overlaid on the difference file. Where all the dark areas were a pink colour indicates a considerable decrease in reflectance that represents a rate of change of -56.24 Km^2/Year. Bright areas with a dark green colour depict a considerable increase in reflectance that represents a rate of change +4.21 Km^2/Year. The rest are set to transparent and therefore grey pixels and white pixels appear in the difference image representing unchanged pixels.

The study area is subject to rapid and increasing changes in LU/LC that result from both natural and human activities and are due to changes in vegetation cover and waterlogging distribution areas. In the current study, according to the results of the analyses, visual interpretation of the enhanced multi-temporal and multi-spectral landsat images spanning 29 years, and also the field verification of the changes in LU/LC do not occur naturally. These are determined by both natural and human impact factors. The determinants of changes in LU/LC of an area are different from the other area. There are many determinants and anthropogenic factors of the changes in LU/

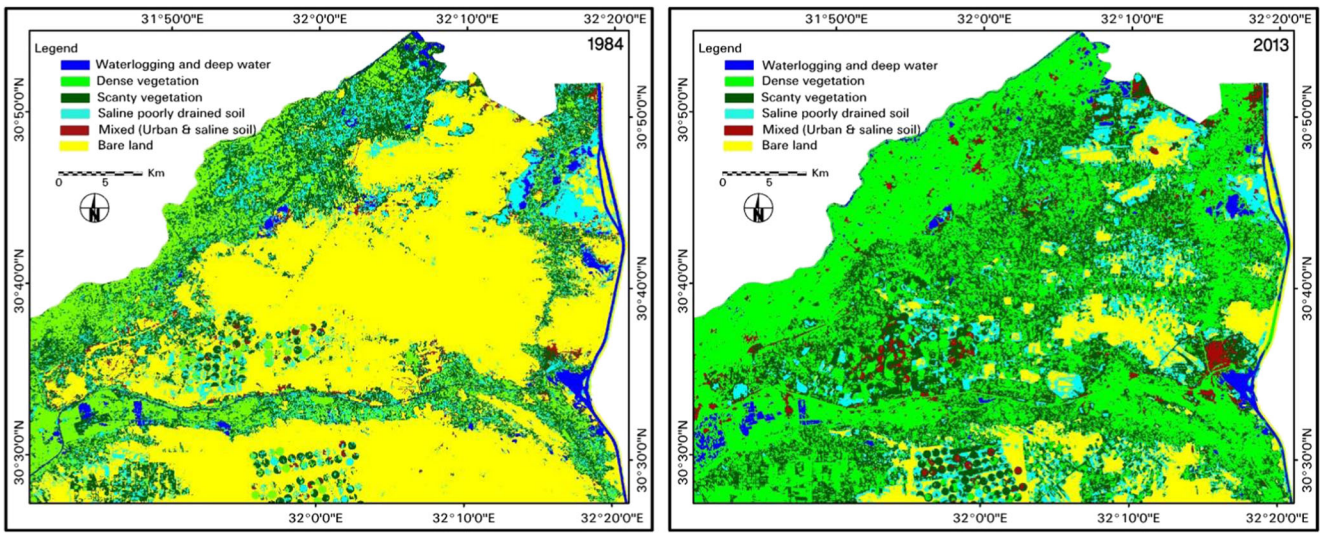

Fig. 17 LU/LC classified Landsat images within timespan 29 years; showing the extension change for different types of classes within the study area

Table 3 Showing the change detection statistical calculations of the LU/LC classes in 1984 and 2013

	1984 (Km^2)	2013 (Km^2)	Rate of change per year	% change to total area
Waterlogged and deep water	61.50	62.20	+0.03	+0.03
Dense vegetation	292.04	1127.04	+28.80	+34.33
Scanty vegetation	434.42	655.50	+7.62	+9.10
Bare land	1284.60	283.40	−34.52	−41.17
Saline poorly drained soil	305.10	227.20	−2.70	−3.21
Mixed (Urban & salt soil)	54.43	76.90	+0.80	+0.92

LC in the study area that are due to land degradation such as; population growth, economic and agricultural sustainable developments, hydrogeological and geological determinants. These multiple functions are the main cause for environmental degradation of the vulnerable resources, especially in arid and semi-arid areas. In the current study area, the prevailing hydrogeological conditions, together with the absence of land-use planning and the lack of a strategy for land reclamation and sustainable developments are mostly responsible for many of the wasteland areas of waterlogging and soil salinization. According to the enhanced data analysis of applying supervised image classification using the maximum likelihood algorithm and then performing the post-classification comparison techniques. The interpretation results of the RS multi-temporal data within time interval 29 year and ancillary geological data the main classes of land resources and activities in the study area are discriminated and classified into six classes with an accuracy of 94 % as; waterlogging and water bodies including canal, drains and lake), dense vegetation and scanty vegetation including Nile deposits, sabkhas and saline poorly drained soil, mixed (urban and saline soil), and bare land including Quaternary deposits (playa, fluviatile, lacustrine deposits and sand dunes) (Fig. 17).

Change detection of LU/LC changes can be classified into high, moderate and low impacts according to the degree of change and wastelands criteria hazards. About 1056.10 Km^2 (43.43 % of total area) of the changes to agricultural activities, including dense and scant vegetation cover in the study area, were due to the development of agriculture and more secondary salinization with an increase the extent of waterlogging and about 1001.2 Km^2 (−41.17 % of total area) of the changes to bare land-use, including Quaternary deposits and sand dunes. Moreover, about 22.50 Km^2 (+0.92 % of total area) of the changes to residential land-use, including urban and villages with some salinization effects in the study area, were due to development of settlements and moreover, due to construction over land-cover of saline soils and bare lands which occur mostly on the desert fringe of the study area. According to the rate of change per year, these activities in the study area are highly environmental impact related to the land-cover in the study area. Generally, the rates of land-use/ land-cover change in the investigated area within time interval of 29 years is shown in Table 3. Vegetation cover - including the dense and scant vegetation cover - is increasing from 726.46 Km^2 in year 1984 to 1782.54 Km^2 in year 2013 at a rate of + 28.80 Km^2/year for dense vegetation and +7.62 km^2/year for scantly vegetation. At the same time, the bare land is decreasing from 1284.60 Km^2 in year 1984 to 283.40 km^2 in year 2013 with a rate of -34.52 km^2/year.

Furthermore, the waterlogging and water bodies are increasing from 61.50 Km^2 in year 1984 to 62.20 km^2 in year 2013 with a rate of +0.03 km^2/ year. These results indicate and reflect a positive correlation between the sustainable agricultural activities in the extended desert fringes and the waterlogging areas. These changes are classified as high impact and include those changes due to the extension and transgression of the study area and due to drowning some cultivated areas by waterlogging followed by salt-affected soils that will occur and the many problems in the infrastructure mainly during the summer season where there are evaporation processes and an increase in temperature. Moreover, other significant rates of changes are produced by the human activities e.g., +0.80 Km^2/Year for residential areas, −2.70 Km^2/Year for sabkhas and Saline poorly drained soil areas. According to the rate of change per year, these activities for agricultural and irrigation sustainable developments in the study area are highly environmental impact related to the land cover in the study area because the main occupation of the people living in this area is agriculture. The agricultural activities and land reclamation projects in this area are intensive. People in this area are trying to cultivate and reclaim more areas in the extended desert fringes. They are modifying the desert fringes of the Nile valleys for agriculture and also capturing the chose area for cultivation. They are trying to sow their crops in every possible area in the region. During the last three decades, the settlements have also been increasing in this area. This trend is found in the whole study area due to high growth rate of population. So, it is natural that settlement will cover more space from the bare and saline lands in the study region. The area under water bodies has increased. Several reservoirs, constructions of irrigation canal, drains and new farms have taken place in recent year. According to Bouwer (1978), Chitale (1991), Mishra et al. (1996) and Kaiser et al. (2013) in irrigated areas, farmers may not be able to control the irrigation that

commonly results in excess water being added to the groundwater. Continued irrigation with excess water leads to a rise in the groundwater table. Waterlogging in low-lying areas is created by the seepage of water from irrigated uplands and from canal system. Excess irrigation by canal water in addition to the inadequate water management practices usually culminates in waterlogging. This is due to many environmental wasteland hazards in the present study area such as flooding of many agricultural lands, infrastructure, houses, industrial zones and electricity towers and also, endangers of accessible railways and asphaltic roads in some areas.

Mitigation measurements of the waterlogged and salinization environmental problems

As revealed by RS and GIS multi-temporal data analyses and interpretations and also the field verification and data collection from the other ancillary geological and hydrogeological data of the study area (Goossens et al. 1993; Geriesh 1994 and 2004; Goossens and Van Ranst 1996; El-Rayes and Geriesh 2003; Mansour 2012; Arnous and El-Rayes 2013; Ghodeif et al. 2013) wastelands created by waterlogging and salt-affected agents reveal and reflect the main causes of waterlogging and soil salinization problems in the investigated study area. These problems relate to canal seepage, faulty irrigation application, geomorphology, inadequate drainage and congestion. Based on the statistical analyses of the change detection and LU/LC calculations; the study area is facing significant changes directly due to human activities including an increase in agricultural, land reclamation and irrigation sustainable developments projects, including approximately 43 % vegetation cover change in the last three decades from the total area In order to make optimal use of these lands and to prevent further degradation. Furthermore, mitigation measures need to be used such as desilting (cleaning) drains more frequently and keeping them free from aquatic vegetation, and all surface drains must be linked to the field drains through link drains to dispose of excess water. This is important as otherwise construction alone will not solve the problem. Use of the ideal quantity of irrigation water should be performed. Moreover, there must be conjunctive and or alternative use of groundwater and canal water in areas where the quality of water is poor which will help in maintaining a favourable salt water balance and the crop yields would be affected to the minimum. Lining and maintaining structure of canals (Ismailia, Port-Said and Suez) and drains (El-Manaif, El-Mahsama, Abu Suwir, Baher El-Baqer, …etc.) network system; it should be assumed to reduce seepage losses to avoid groundwater level and waterlogging impact hazards. Finally, it is important to educate and raise awareness amongst the local farmers about the misuse of irrigation applied by flooding and the need for scientific practices of irrigation. Where irrigated water is penetrating through the soil profile and contains a majority of the salts left behind by evaporation and transpiration phenomenon. As the water moves through the soil profile it may carry extra salts by dissolution and some salts may precipitate out in the soil; whereas others will be exchanged with some salt ions in the water applied to the land; and also due to the degradation of the water quality. Moreover, salt-resistant crops and / or horticultural plantation types only should be grown in the study area.

Conclusions

Waterlogging and salt-affected wasteland indicators, either naturally occurring or human induced, are serious global environmental hazard problems that go hand in hand, mainly in arid and semi-arid regions. These are a complex and dynamic process with serious consequences for geo-environmental conditions as well as, geomorphological, hydrological, climatic, agricultural, and socio-economic impacts. The monitoring, assessment and mapping of its extent and severity at an early stage become very important at both local and regional scales. In the current study, a number of different ways of mapping, monitoring and predicting waterlogged and salt-affected land have been used, all of which have strengths and weaknesses. The most suitable solutions to produce the best results for monitoring, assessing and mapping the waterlogged and salt-affected areas were achieved by using multi-temporal Landsat 5, 7 and 8 data in 1984, 2000, 2006 and 2013; and then apply the digital image processing and enhancement such as band combination, PCA, change detection and image classification techniques and also many indices such as NDVI, NDSI, NDWI and NDBI. All of them were successes help to construct various thematic and spatial distribution change maps of these hazard indicators. The main difficulty in the retrieval of salt-affected areas from satellite data is to discriminate between urban and salt classes; but this can be overcome by excluding the confused areas by digitizing from the statistical calculation processes. The optimal time period for acquiring RS data to monitor and assess salt-affected area in the investigated area with the NDVI, NDSI and NDBI indices is March to avoid any spectral confusion of pixel mixing with urban areas that is occurring in peek summers times. In addition, the PCA technique shows promising potential in identifying and discriminating between all different classes in the study area particularly the hydrosalinized wastelands such as the permanent, temporary waterlogged, salt-affected areas, bare land and vegetation.

Based on image interpretation and field observations - using ERDAS Imagine and ArcGIS to identify and estimate the dynamic changes of surface waterlogging and salt-affected - areas were delineated and mapped as digital layers. The results of the integration process of these layers by using ArcGIS functions are revealed and it is estimated that between 11 and 77 Km^2 of area are affected by seasonal and permanent waterlogging respectively. Moreover, it is estimated that

85 Km^2 areas of saline soil (dry saline or saturated saline soils) from 1984 to 2013 respectively. A reduction of 173 Km^2 wasteland area especially in classes like permanent and temporary waterlogged are identify and delineated in multi-temporal vector layers. Moreover, change detection results for the waterlogged areas during the years 1984–2013 indicate that its surface area increased about 28 Km^2 and decreased about 29 Km^2. At the same time, the salt-affected surface areas increased about 50 Km^2 and decreased about 45 Km^2. Landform, water table, depth to water, slope and elevation spatial data are considered to be controlling factors in the study area due to an increase or decrease in many environmental impacts. Therefore, the current study successfully shows that mapping the relationship between them will reveal that any hotspot area will be suffering from waterlogging and then the effects of salt. Image classification and change detection techniques were applied in the present study to construct the LU/LC map and to determine the rate of change in the study area. The post-classification comparison results show that the vegetation cover including the dense and scantly vegetation is increasing from 726 Km^2 in year 1984 to 1783 Km^2 in year 2013 with a rate of +29 Km^2/year for dense vegetation and + 7.6 km^2/year for scantly vegetation. At the same time, the bare land is decreasing from 1284 Km^2 in year 1984 to 283 km^2 in year 2013 with a rate of -35 km^2/year. Furthermore, waterlogging and water bodies are increasing from 61 Km^2 in year 1984 to 62 km^2 in year 2013 with a rate of +0.03 km^2/year. These results indicate and reflect a positive correlation between sustainable agricultural activities and land reclamation in the extended desert fringes and the waterlogging areas. Finally, the study introduces mitigation measurements based on the results and the main causes of the wasteland and environmental hazards; and may well prevent any sustainable developments in the future. Therefore, it is becoming urgent that decision-makers now undertake a series of informed actions concerning recommended mitigation measurements from the present study that will enable the best possible solution when the current environmental emergency ultimately passes.

Acknowledgments The authors wish to acknowledge the funding support provided by the Science and Technology Development Fund (STDF), Ministry of Scientific Research, Egypt - project number 6084, which has made this research possible.

References

Al-Abdulghani E, El-Sammak A, Sarawi M (2013) Environmental assessment of Kuwait Bay: an integrated approach. J Coast Conserv 17:445–462. doi:10.1007/s11852-013-0242-7

Allbed A, Kumar L (2013) Soil salinity mapping and monitoring in arid and semi-arid regions using remote sensing technology: a review. Adv Remote Sens 2:373–385

Anonymous (1976) Report of the national commission on agriculture, part V, IX and abridged report Ministry of Agriculture and Irrigation, Government of India, New Delhi

Arnous MO (2011) Integrated remote sensing and GIS techniques for landslide hazard zonation: a case study Wadi Watier area, South Sinai, Egypt. J Coast Conserv 15(4):477–497. doi:10.1007/s11852-010-0137-9

Arnous MO, El-Rayes AE (2013) An integrated GIS and hydrochemical approach to assess groundwater contamination in West Ismailia area, Egypt. Arab J Geosci 6(8):2829–2842. doi:10.1007/s12517-012-0555-0

Arnous MO, Green DR (2011) GIS and remote sensing as tools for conducting geo-hazards risk assessment along Gulf of Aqaba coastal zone, Egypt. J Coast Conserv 15(4):457–475. doi:10.1007/s11852-010-0136-x

Arnous MO, Aboulela HA, Green DR (2011) Geo-environmental hazards assessment of the north western Gulf of Suez, Egypt. J Coast Conserv 15(1):37–50. doi:10.1007/s11852-010-0118-z

Bouwer H (1978) Groundwater Hydrology, In: McGraw-Hill Series in Water Resources and Environmental Engineering, Library of Congress, Washington DC, pp. 294-299

Bouwer H, Dedric AR, Jaynes DB (1990) Irrigation management for ground flood hazards vulnerability and risk assessment in Indo Gangetic plain. Nat Hazards. doi:10.1007/s11069-010-9525-6

Chaube VK (1998) Assessment of waterlogging in Sriram Sagar command area, India, by remote sensing. Water Resour Manag 12(5): 343–357

Chavez PS Jr (1996) Image-based atmospheric corrections-revisited and improved. Photogramm Eng Remote Sens 62:1025–1035

Chen S, Rao P (2008) Land degradation monitoring using multi-temporal landsat TM/ETM data in transition zone between grassland and cropland of northeast China. Int J Remote Sens 29(7):2055–2073

Chikhaoui M, Bonn F, Bokoye AI, Merzouk A (2005) A spectral index for land degradation mapping using ASTER data: application to a semi-arid Mediterranean catchment. Int J Appl Earth Obs Geoinformation 7(2):140–153

Chitale MA (1991) Environmental management in water resources project – Indain experiences of irrigation power project. J Indain Water Res Soc 1(2):56–59

Deering D, Rouse J (1975) Measuring 'Forage Produc-tion' of Grazing Units from Landsat MSS Data. 10th International Symposium on Remote Sensing of Environment, ERIM, Ann Arbor, pp. 1169-1178

Dwivedi RS (1994) Study of salinity and waterlogging in Uttar Pradesh (India) using remote sensing data. Land Degrad Rehabil 5:191–199

Dwivedi RS, Sreenivas K (1998a) Delineation of salt affected soils and waterlogged areas in the Indo-Gangetic Plains using IRS-IC LISS III data. Int J Remote Sens 19(14):2739–2751

Dwivedi RS, Sreenivas K (1998b) Image transforms as a tool for the study of soil salinity and alkalinity. Int J Remote Sens 19:506–610

Dwivedi RS, Sreenivas K, Ramana KV (1999) Inventory of salt-affected soils and waterlogged areas: a remote sensing approach. Int J Remote Sens 20:1589–1599

Dwivedi RS, Ramana KV, Thammappa SS, Singh AN (2001) The utility of IRS-1C and LISS-III and PAN-Merged data for mapping salt-affected soils. Photogramm Eng Remote Sens 67(10):1167–1175

Egyptian Meteorological Authority (2006) Climatic Atlas of Egypt. Published., Arab Republic of Egypt, Ministry of Transportation and communications

El Baroudy AA, Moghanm FS (2014) Combined use of remote sensing and GIS for degradation risk assessment in some soils of the Northern Nile Delta, Egypt. Egyptian J Remote Sens Space Sci 17:77–85

Elnaggar AA, Noller JS (2009) Application of remote- sensing data and decision-tree analysis to mapping salt- affected soils over large areas. Remote Sens 2(1):151–165

El-Rayes AE, Geriesh MH (2003) Reasons of groundwater logging around Sarabiuem Waste water treatment Plant, Ismailia, Egypt. 5th International Conference of Groundwater rising control in the residential areas, Mansoura Univ., Egypt

El-Shazly EM, Abd El-Hady MA, El-Shazly MM, El-Kassas IA, El-Ghawaby MA, Salman AB, Morsi MA (1975) Geology and groundwater potential studies of El Ismailia master plan study area. Remote Sensing Research Project, Academy of Scientific Res. and Techno., Cairo, Egypt

Faust NL (1989) In: Kent A, Williams JG (eds) Image Enhancement. Vol. 20, Supplement 5 of Encyclopedia of Computer Science and Technology. Marcel Dekker, Inc, New York

Fernandez-Buces N, Siebe C, Cram S, Palacio JL (2006) Mapping soil salinity using a combined spectral res- ponse index for bare soil and vegetation: a case study in the former lake Texcoco, Mexico. J Arid Environ 65(4):644–667

Furby SL (1995) Detecting and monitoring salt-affected land: a report from the LWRRDC project detecting and monitoring changes in land condition through time using remotely sensed data, Remote Sensing and Image Integration Group. CSIRO Division of Mathematics & Statistics, Perth

Gao J, Liu Y (2008) Mapping of land degradation from space: a comparative study of Landsat ETM+ and ASTER data. Int J Remote Sens 29(14):4029–4043

Gao J, Liu Y (2010) Determination of land degradation causes in Tongyu County, Northeast China via land cover change detection. Int J Appl Earth Obs Geoinformation 12:9–16

Geriesh MH (1994) Hydrogeological and hydrogeochemical evaluation of groundwater resources in Suez canal region. Ph.D. thesis, Fac. Sci., Suez Canal Univ., Ismailia, Egypt

Geriesh MH (2004) Land degradation and soil salinization due to water logging in the newly reclaimed areas, East of Bitter Lakes, Sini Peninsula, Egypt. 7th Conf. Geol. Sinai Develop., Ismailia, Egypt, pp. 23-40

Ghodeif KO, Arnous MO, Geriesh MH (2013) Define a protected buffer zone for Ismailia Canal, Egypt using Geographic Information Systems. Arab J Geosci 6(1):43–53. doi:10.1007/s12517-011-0326-3

Goossens R, Van Ranst E (1996) The use of remote sensing and GIS to detect gypsiferous soils in the Islamic Province (Egypt), Proceeding of the International Symposium on Soils with Gypsum. Lleida, 15–21 September, 1996.Catalonaia, Spain

Goossens, R., De Dapper, M., Gad, A., Ghabour, Th., 1993. A model for monitoring and prediction of soil salinity and waterlogging in the Ismailia area (Egypt) based on remote sensing and GIS. In: Proceedings of the International Symposium on Operationalization of Remote Sensing, vol. 6, ITC Enschede, The Netherlands, pp. 97–107

Haboudane D, Bonn F, Royer A, Sommer S, Mehl W (2002) Land degradation and erosion risk mapping by fusion of spectrally-based information and digital geomorphometric attributes. Int J Remote Sens 23:3795–3820

Hadeel AS, Jabbar MT, Xiaoling C (2011) Remote sensing and GIS application in the detection of environmental degradation indicators. Geo-spatial Inf Sci 14(1):39–47

Hill J, Sommer S, Mehl W, Megier J (1995) Use of Earth observation satellite data for land degradation mapping and monitoring in Mediterranean ecosystems: towards a satellite-observatory. Environ Monit Assess 37(1–3):143–158

Jabbar MT, Chen X (2008) Land degradation due to salinization in arid and semi-arid regions with the aid of geo-information techniques. Geo-Spatial Inf Sci 11(2):112–120

Jensen JR (2004) Introductory digital image processing: a remote sensing perspective. Prentice-Hall, Englewood Cliffs

Juman RA, Ramsewak D (2013) Land cover changes in the Caroni Swamp Ramsar Site, Trinidad (1942 and 2007): implications for management. J Coast Conserv 17:133–141. doi:10.1007/s11852-012-0225-0

Kaiser MF, El-Rayes A, Ghodeif K, Geriesh B (2013) GIS data integration to manage waterlogging problem on the eastern nile delta of Egypt. Int J Geosci 4:680–687

Khalifa IH, Arnous MO (2012) Assessment of hazardous mine waste transport in west central Sinai, using remote sensing and GIS approaches: a case study of Um Bogma area, Egypt. Arab J Geosci 5(3):407–420. doi:10.1007/s12517-010-0196-0

Khan NM, Rastoskuev VV, Sato Y, Shiozawa S (2005) Assessment of hydrosaline land degradation by using a simple approach of remote sensing indicators. Agric Water Manag 77:96–109

Li XJ, Wang Z, Song K, Zhang B, Liu D, Guo Z (2007) Assessment for salinized wasteland expansion and land use change using GIS and remote sensing in the West part of Northeast China. Environ Monit Assess 131(1–3):421–437

Lu D, Batistella M, Mausel P, Moran E (2007) Mapping and monitoring land degradation risks in the Western Brazilian Amazon using multitemporal Landsat TM/ETM+ images. Land Degrad Dev 18: 41–54

Mandal AK, Sharma RC (2001) Mapping waterlogged areas and salt-affected soils in the IGNP command area. J Indian Soc Remote Sens 29(4):229–235

Mandal AK, Sharma RC (2011) Delineation and characterization of waterlogged salt affected soils in IGNP using remote sensing and GIS. J Indian Soc Remote Sens 39(1):39–50

Mansour BM (2012) Management of groundwater logging problems along Wadi El-Tumilat, Eastern Nile Delta using mathematical modeling and GIS techniques. M.Sc. thesis, Fac. Science, Suez Canal Univ., Ismailia, Egypt. 220p

Mas JF (1999) Monitoring land-cover changes: a comparison of change detection techniques. Int J Remote Sens 20(1):139–152

McFarlane Don J, George RJ, Caccetta PA (2004) The extent and potential area of salt-affected land in Western Australia estimated using remote sensing and digital terrain models [online]. In: Dogramaci, Shawan (Editor); Waterhouse, Alex (Editor). Engineering Salinity Solutions : 1st National Salinity Engineering Conference 2004. Barton, A.C.T: Engineers Australia, 2004: 55–60

Mcffers SK (1996) The use of the normalized difference water index (NDWI) in the delineation of open water features. Int J Remote Sens 17:1425–1432

Metternichit G, Zinck JA (1997) Spatial discrimination of salt- and sodium-affected soil surfaces. Int J Remote Sens 18(12):2571–2586

Mishra GC, Kumar B, Shukla M (1996) Subsurface drainage investigation in stage II of Indira Gandhi Nahar Pariyojna at RD 38, Technical Report, National Institute of Hydrology

Mouat DA, Mahin GG, Lancaster J (1993) Remote sensing techniques in the analysis of change detection. Geocarto Int 8(2):39–50

Nosair AM (2011) Climatic changes and their impacts on groundwater occurrence in the northern part of east Nile Delta, Egypt. M.Sc. thesis, Zagazig Uni., Egypt

Pandey AC, Singh S, Kumar NON, Nathawat MS (2010) Water logging and water quality protection. Irrig Drain Syst 4:375–383

Phinn S, Stanford M (2001) Monitoring land-cover and land-use change in a rapidly urbanising coastal environment:the Maroochy and Mooloolah Rivers catchments, southeast Queensland, 1988-1997. Aust Geogr Stud 39(2):217–232

Prince SD, Becker-Reshef I, Rishmawi K (2009) Detection and mapping of long term land degradation using local net production scaling: application to Zimbabwe. Remote Sens Environ 113: 1046–1057

Purevdorj R, Tatelshi T, Ishiyama Y (1998) Relationships between percent vegetation cover and vegetation indices. Int J Remote Sens 19(18):3519–3535

Raina P, Joshi DC, Kolarkar AS (1993) Mapping of soil degradation by using remote sensing on alluvial plain, Rajasthan, India. Arid Soil Res Rehabitition 7(2):145–161

Rubec CD, Thie J (1980) Land use monitoring with Landsat digital data in southwestern Manitoba. Ed: MacEwan, A. In Proc. 5th Canadian symposium on remote sensing, Victoria BC, August 1978. (Canadian Aeronautics and Space Institute, Ottawa), pp. 136-149

Runnstrom MC (2003) Rangeland development of the Mu Us Sandy Land in semiarid China: an analysis using Landsat and NOAA remote sensing data. Land Degrad Dev 14:202

Sabins FF (1997) Remote sensing principles and interpretation, 3rd edn. W: H: Freeman and Company, New York, p 449

Singh A (2015) Soil salinization and waterlogging: a threat to environment and agricultural sustainability. Ecol Indic 57:128–130

Singh A, Panda SN, Flugel W, Krause P (2012) Waterlogging and farmland salinization: causes and remedial measures in an irrigated semiarid region of India. Irrig Drain. doi:10.1002/ird.651

Sujatha G, Dwivedi RS, Sreenivas K, Venkataratnam I (2000) Mapping and monitoring of degraded lands in part of Jaunpur district of Uttar Pradesh using temporal spaceborne multispectral data. Int J Remote Sens 21:519–531

Symeonakis E, Drake N (2004) Monitoring desertification and land degradation over sub-Saharan Africa. Int J Remote Sens 25: 573–592

Tripathi NK, Rai BK, Dwivedi P (1997) Spatial modeling of soil alkalinity in GIS environment using IRS data. The 18th Asian Conference on Remote Sensing, Kualalampur

Van Lynden GWJ, Mantel S (2001) The role of GIS and remote sensing in land degradation assessment and conservation mapping: some user experiences and expectations. Int J Appl Earth Obs Geoinformation 3:61–68

Zhao HM, Chen XL (2005) Use of normalized difference bareness index in quickly mapping bare areas from TM/ETM+. Geosci Remote Sens Symp 3(25–29):1666–1668